Available online at www.sciencedirect.com
ScienceDirect
Biochemical and Biophysical Research Communications 352 (2007) 164–169
BBRC
www.elsevier.com/locate/ybbrc

A novel embryotoxic estimation method of VPA using ES cells differentiation system

Mayu Murabe, Junji Yamauchi, Yoko Fujiwara, Masami Hiroyama, Atsushi Sanbe, Akito Tanoue *

Department of Pharmacology, National Research Institute for Child Health and Development, Setagaya, Tokyo 157-8535, Japan

Received 26 October 2006
Available online 13 November 2006

Abstract

Valproic acid (VPA), which has a wide range of therapeutic applications, is known as a potent teratogen that induces neural tube defects in vertebrates. Here, we have characterized the tissue-specific, embryotoxic effects of VPA on developmental processes using a novel system with differentiating mouse ES cells. Under our cultivating condition, ES cells differentiated into cardiomyocytes, although various cell types can be differentiated. VPA affected cell viability and differentiation from undifferentiated ES cells to cardiomyocytes in a dose-dependent manner. The analysis of tissue-specific markers also revealed that VPA potently inhibited mesodermal and endodermal development but promoted neuronal differentiation in a lineage-specific manner. Taking the *in vivo* teratogenicity of VPA into account, this assay system could be useful in predicting the degree of embryotoxicity of VPA. We, thus, propose that the *in vivo* embryotoxic effects of various medicines can be estimated fast and accurately using this *in vitro* cell differentiation system.

Keywords: ES cell; Valproic acid; Embryotoxicity

Valproic acid (VPA) is a short-chained fatty acid with a broad spectrum of antiepileptic activities and it is also used in migraine prophylaxis and the treatment of bipolar disorders, neuropathic pain [1,2]. It is also being tried as an anticancer agent. VPA, which has a wide range of therapeutic applications, is also a potent teratogen and is associated with elevated risks for neural, craniofacial, cardiovascular, and skeletal birth defects [3,4]. The predominant VPA-induced teratogenic effects are due to failure of the neural tube to close (neural tube defects, NTDs), leading to conditions such as spina-bifida-aperta, anencephaly, and exencephaly in humans, mice, and other vertebrates [3,5–7].

In this study, we attempted to characterize the tissue-specific embryotoxicity of VPA using a system with mouse embryonic stem (ES) cell differentiation. This *in vitro* embryotoxicity assay requires a simple procedure that can be accomplished in a shorter time (10 days) [8] than that required by other assays used in developmental toxicological studies with experimental animals. Since ES cells are undifferentiated pluripotent embryo-derived stem cell lines and are capable to develop into differentiated cell types representing endodermal, ectodermal, and mesodermal lineages, ES cells lines are very suitable to analyze the mutagenic, cytotoxic, and embryotoxic effects of chemical compounds *in vitro* [9]. By analyzing the expression of tissue-specific genes and conducting histological and immunocytochemical studies, we have demonstrated that VPA inhibits the differentiation of mesodermal and endodermal lineages. On the other hand, VPA can induce neural differentiation in a lineage-specific manner. It is conceivable that these abnormalities of tissue developments in ES cells reflect the embryotoxic effects of VPA *in vivo*. Using this *in vitro* embryotoxicity estimation system, it would be possible to predict the effects of chemicals on developmental processes *in vivo* in a short time.

* Corresponding author. Fax: +81 3 5494 7057.
E-mail address: atanoue@nch.go.jp (A. Tanoue).

0006-291X/$ - see front matter © 2006 Elsevier Inc. All rights reserved.
doi:10.1016/j.bbrc.2006.10.189

Materials and methods

Materials. The following antibodies were purchased: anti-troponin I from Chemicon (Temecula, CA), anti-albumin from Bethyl Laboratory (Montgomery, TX), and anti-neurofilament 200 from Sigma–Aldrich (St. Louis, MO).

ES cell culture. Mouse ES cells (R1) were maintained and used for differentiation as previously described [10]. ES cells were grown on 0.1% gelatin-coated tissue culture dishes in a standard ES-cell culture medium-containing D-MEM supplemented with 10% FCS, 2 mM glutamine, 0.1 mM non-essential amino acids, 0.1 mM β-mercaptoethanol, 1000 U/ml LIF (Chemicon, Temecula, CA), 50 U/ml penicillin G, and 50 μg/ml streptomycin. For the differentiation of R1 ES cells, we followed the method of the embryonic stem cell test (EST) [8]. In brief, ES cells were suspended in an ES-differentiation medium-containing D-MEM supplemented with 20% FCS, 2 mM glutamine, 0.1 mM non-essential amino acids, 0.1 mM β-mercaptoethanol, 50 U/ml penicillin G, and 50 μg/ml streptomycin and cultivated in hanging drops ($n = 500$) as aggregates (called embryoid bodies (EBs)) for 3 days [10]. The EBs were transferred to suspension culture dishes (Sumitomo Bakelite, Tokyo, Japan) and cultured for 2 days. They ($n = 1$/well) were plated onto a 24-well tissue culture plate on day 5 and incubated for 5 additional days. To estimate the differentiating efficiencies from ES cells into cardiomyocytes, the distinctive beating movements of differentiated cardiomyocytes were analyzed under an inverted phase-contrast microscope (Nikon, Tokyo, Japan).

Cytotoxicity assay. For the cytotoxicity assay, we followed the method of the embryonic stem cell test (EST) [8]. ES cells and NIH-3T3 fibroblasts (1×10^4 cells/ml) were seeded in a volume of 50 μl/well into a 96-well flat-bottomed tissue culture microtiter plate and incubated in a humidified atmosphere with 5% CO_2 at 37 °C for 2 h. After incubation, 150 μl of a culture medium-containing the appropriate dilution of test chemicals was added. On day 3 and day 5, the culture medium was removed, and, subsequently, 200 μl of the same concentration of the test substance used on day 1 was added to the microtiter plates. On day 10, the methylthiazolyldiphenyl-tetrazolium bromide (MTT) cytotoxicity assay [11] was carried out [8]. A volume of 20 μl of 5 mg/ml 3-[4,5-dimethylthiazol-2-yl]-2,5-diphenyl-tetrazolium bromide, MTT (Sigma–Aldrich, St. Louis, MO), in PBS was added into each microtiter well and incubated in a humidified atmosphere with 5% CO_2 at 37 °C for 2 h. After removal of the supernatant, cells were incubated with 130 μl of a desorb-mix solution-containing 3.49% (v/v) of a 20% SDS aqueous solution and 96.51% (v/v) 2-propanol. After agitation for 15 min on an N-704 microtiter plate shaker (Nissin, Tokyo, Japan), the plates were transferred to a Wallac 1420 multilabel counter (Perkin-Elmer, Wellesley, MA), and the absorbance of each well at a wavelength of 520 nm and a reference wavelength of 630 nm was examined. Representative results from three separate experiments are shown in the figure. For morphological observations, samples on day 5 were examined using a Hoffman differential interference contrast microscope.

Immunocytochemistry. On day 3 of the differentiation assay, several EBs were cultured on 0.1% gelatin-coated glass-based 60 mm dishes. After changing the media on day 5, the cells of day 10 were fixed with 4% paraformaldehyde for 20 min at room temperature. After rinsing with PBS twice, samples were pretreated with PBS-containing 0.2% Triton X-100 in PBS for 30 s. After washing with PBS twice, the samples were incubated with PBS-containing 0.1 M glycine, pH 3.5, for 30 min, rinsed with PBS twice, and blocked in PBS-containing 1% BSA, 0.1% gelatin, and 0.1% Tween 20 for 1 h at room temperature. They were incubated at 4 °C overnight with the following antibodies: anti-troponin I (mouse IgG, 1:500), anti-albumin (goat IgG, 1:500), and anti-neurofilament 200 (rabbit IgG, 1:500). After washing with PBS three times, the cells were incubated for 1 h at room temperature with secondary antibodies conjugated with Alexa 488 (Invitrogen, Carlsbad, CA). After washing with PBS three times, the samples were mounted with the Vectashield mounting medium with DAPI (Vector Laboratories, Burlingame, CA) and examined with an FV500 confocal laser scanning microscope (Olympus, Tokyo, Japan). To estimate the differentiating efficiencies from ES cells into neuronal cells, NF-positive cells (neurons) were counted against DAPI-positive cells (~200 cells) under an inverted phase-contrast microscope (Nikon, Tokyo, Japan). Representative results from three separate experiments are shown in the figure.

RNA isolation, cDNA synthesis, and RT-PCR. Total RNA was extracted from samples on day 10 of the differentiation assay using the RNA extraction kit ISOGEN (Nippon Gene, Tokyo, Japan) and digested with deoxyribonuclease (RT Grade) (Nippon Gene, Tokyo, Japan) to remove any contaminating genomic DNA. The concentration of RNA was measured with a BioSpec-mini DNA/RNA/protein analyzer (Shimazu, Kyoto, Japan). cDNA was synthesized with the use of 3 μg of RNA, 500 ng of oligo-dT12-18 primers, and 200 U of SuperScript III reverse transcriptase (Invitrogen, Carlsbad, CA). To analyze the relative expression of different mRNAs, the amount of cDNA was normalized on the basis of the signals from ubiquitously expressed β-actin mRNA. PCR was carried out using an Ex-Taq kit (Takara Bio, Shiga, Japan) according to the manufacturer's standard protocol in a final volume of 25 μl. The primer sequences are summarized in Table 1.

Table 1
PCR primers for the detection of tissue-specific marker gene expressions used in this study

Gene	Sequences (5′–3′)		Product length (bp)
	Forward	Reverse	
Oct4	GGTGGAGGAAGCCGACAAC	TTCGGGCACTTCAGAAACATG	141
Sox2	AGATGCACAACTCGGAGATCAG	CCGCGGCCGGTATTTATAAT	146
BMP4	CTGCCGTCGCCATTCACTAT	TGGCATGGTTGGTTGAGTTG	146
Nkx2.5	CCAAGTGCTCTCCTGCTTTCC	CCATCCGTCTCGGCTTTGT	148
MLC-2v	GCTTCATCGACAAGAATGAC	GAATGCGTTGAGAATGGTCT	185
ANF	CGGTGTCCAACACAGATCTG	TCTCTCAGAGGTGGGTTGAC	187
MyoD	ACGGCTCTCTCTGCTCCTTTG	CGTGCTCCTCCGGTTTCA	138
GATA6	CGGTCATTACCTGTGCAATG	GCATTTCTACGCCATAAGGTA	159
TTR	GTCCTCTGATGGTCAAAGTC	TCCAGTTCTACTCTGTACAC	193
HNF1	AGCCGCAGAACCTTATCATG	GGTTGGTGTCTGTGATCAAC	390
AFP	ACTCACCCCAACCTTCCTGTC	CAGCAGTGGCTGATACCAGAG	422
ALB	GGAACTTGCCAAGTACATGTGTGA	CAGCAATGGCAGGCAGATC	146
Nestin	TGCATTTCCTTGGGATACCAG	CTTCAGAAAGGCTGTCACAGGAG	122
Synaptophysin	GTGGAGTGTGCCAACAAGAC	ATTCAGCCGAGGAGGAGTAG	158
NFH	AGGACCGTCATCAGGCAGACATTGC	GACCAAAGCCAATCCGACACTCTTC	201
GFAP	TGCCACGCTTCTCCTTGTCT	GCTAGCAAAGCGGTCATTGAG	146
Olig2	TGCGCCTGAAGATCAACAG	CATCTCCTCCAGCGAGTTG	182
DM20	TGAAGCTCTTCACTGGTACAG	GTCTTGTAGTCGCCAAAGAT	207
β-Actin	GCTCTGGCTCCTAGCACCAT	GGGCCGGACTCATCGTACT	146

Quantitative RT-PCR. For quantitative RT-PCR, gene expression was assessed by real-time PCR with the use of a 7900HT Fast Real-Time PCR System (Applied Biosystems, Foster City, CA). The reaction mixtures contained 1 μl of template cDNA with 100 nM of forward and reverse primers and 10 μl of SYBR Premix Ex Taq (Takara Bio, Shiga, Japan) in a total volume of 20 μl. Duplicate assays were run for each sample, and each included a standard curve and a negative control. Specific oligonucleotide primers were designed to produce 122- to 422-bp products. The amplification protocol consisted of 10 min at 95 °C followed by 40 cycles at 95 °C for 15 s and 60 °C for 1 min. The relative quantitative expressions of tissue-specific markers, after normalization with GAPDH as a housekeeping gene, were calculated. The primer sequences are summarized in Table 1. The primers for GAPDH were purchased from Applied Biosystems (Foster City, CA).

Results

The cell viability assay (MTT assay) was used to study the cytotoxic effect of VPA with ES cells, representing embryonic tissues, and NIH-3T3 fibroblasts, representing adult tissues. In both cell lines, VPA inhibited the survival of cells in a dose-dependent manner (Fig. 1). However, there was a significant difference in cytotoxic sensitivities against VPA between ES cells and NIH-3T3 fibroblasts. The IC_{50} values, the inhibitory concentration of 50% cell viability, were calculated at 3.25 and 0.56 mM for NIH-3T3 fibroblasts and ES cells, respectively. The therapeutic range of VPA is 0.30–0.70 mM in serum. The IC_{50} value of NIH-3T3 fibroblasts, 3.25 mM, was approximately 5–11 times the therapeutic concentration. In contrast, the IC_{50} of ES cells, 0.56 mM, was within the therapeutic range of VPA. Since ES cells are more significantly affected by the therapeutic range of VPA than NIH-3T3 fibroblasts, developing cells during embryogenesis could be seriously damaged by the VPA therapeutic concentration. To observe the cytotoxic and morphological effects of VPA on ES cells and NIH-3T3 fibroblasts, ES cells and NIH-3T3 fibroblasts colored with the MTT were observed on day 5 of the cytotoxicity assay (Fig. 1). In both cell lines, the cell densities were gradually reduced in a concentration-dependent manner. In a high-medication group, NIH-3T3 fibroblasts showed strong indications of shrinking. However, in ES cells, many small cells, considered as undifferentiated cells, showed strong signs of inhibition to differentiation.

To characterize the tissue-specific effects of VPA on the ES differentiation system at the molecular levels, the expression levels of typical tissue-specific genes were examined using RT-PCR analysis with samples on day 10 of the differentiation assay (Supplemental Fig.1). In this culture condition-containing 20% FCS, ES cells were mainly differentiated into endodermal and mesodermal lineages, such as cardiomyocytes, but not into ectodermal lineages, such as neural cells. This is in agreement with the fact that some growth factors involved in FCS are known to inhibit the neural induction of various kinds of adult neural stem cells. Oct4, a representative undifferentiated marker, was highly detected in all samples of high VPA concentrations. Other primitive markers, such as BMP4 (a mesodermal marker), GATA6 (an endodermal marker), and Nestin (an ectodermal, neural marker), were also strongly detected in the samples with high VPA concentrations. In contrast, VPA reduced the expression levels of late-stage markers, such as Nkx2.5 and MLC-2v (cardiomyocyte markers) and TTR, HNF1, AFP, and albumin (ALB) (endodermal markers), whereas Synaptophysin (Syn), a typical neural marker, was increased in a VPA concentration-dependent manner. No expression of MyoD (a muscle marker) and GFAP (a glial marker) was detected. These results suggest a tendency for VPA to inhibit the differentiation into

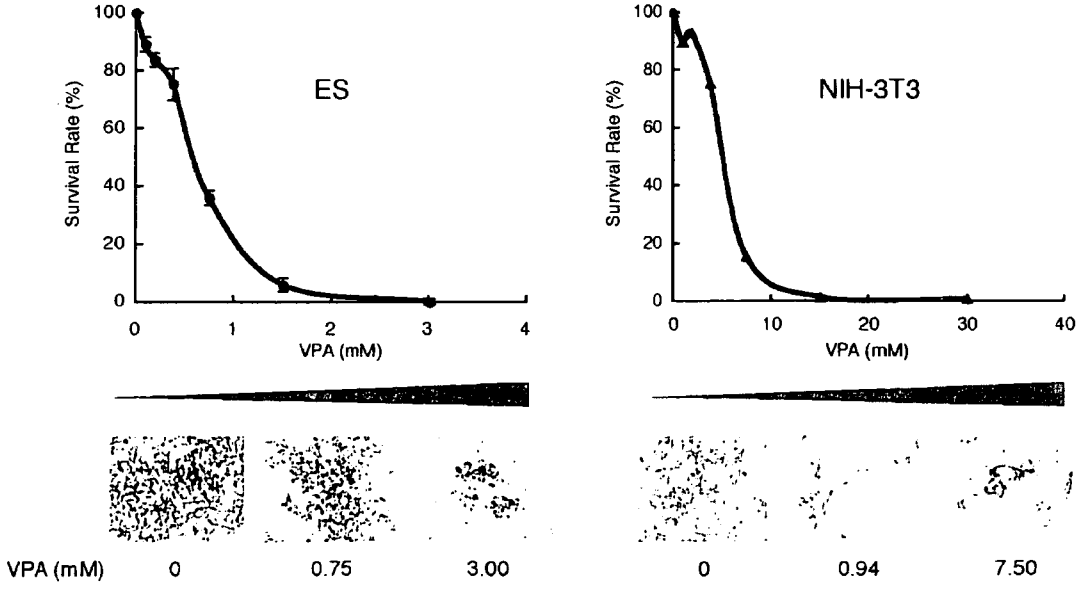

Fig. 1. Cytotoxicity assay for ES cells and NIH-3T3 fibroblasts. Cells on day 10 of the assay were stained with the MTT and solubilized. The activity of the mitochondrial enzyme of living cells was examined. The violet color of the MTT formazan, which is the enzyme product, was measured with the absorbance of 520 nm. On day 5, cells were stained with the MTT and examined with a Hoffman differential interference contrast microscope.

cardiomyocytes and endodermal lineages and to adversely induce differentiation into neural lineages. Undifferentiated ES cells also remained under a condition of high VPA concentration.

To characterize the VPA effects more closely, we performed quantitative expression analysis of tissue-specific genes and immunocytochemical or morphological analysis with samples on day 10 of the differentiation assay (Figs. 2 and 3). It was demonstrated that the expression levels of Oct4 and Sox2 (undifferentiated markers) were high under the condition of high VPA concentration (Fig. 2A-(1)). For mesodermal lineages, the expressions of BMP4, Nkx2.5, MLC-2v, and ANF were reduced, and MyoD was not detected (Fig. 2A-(2)). On day 10 of the differentiation assay, cardiomyocytes were normally differentiated (Fig. 2C, left). The number of cells stained with an antibody against troponin I (a typical cardiomyocyte-specific marker) was decreased notably under the conditions of high VPA concentration (data not shown). The ratio of induced cardiomyocytes was determined from their autonomous

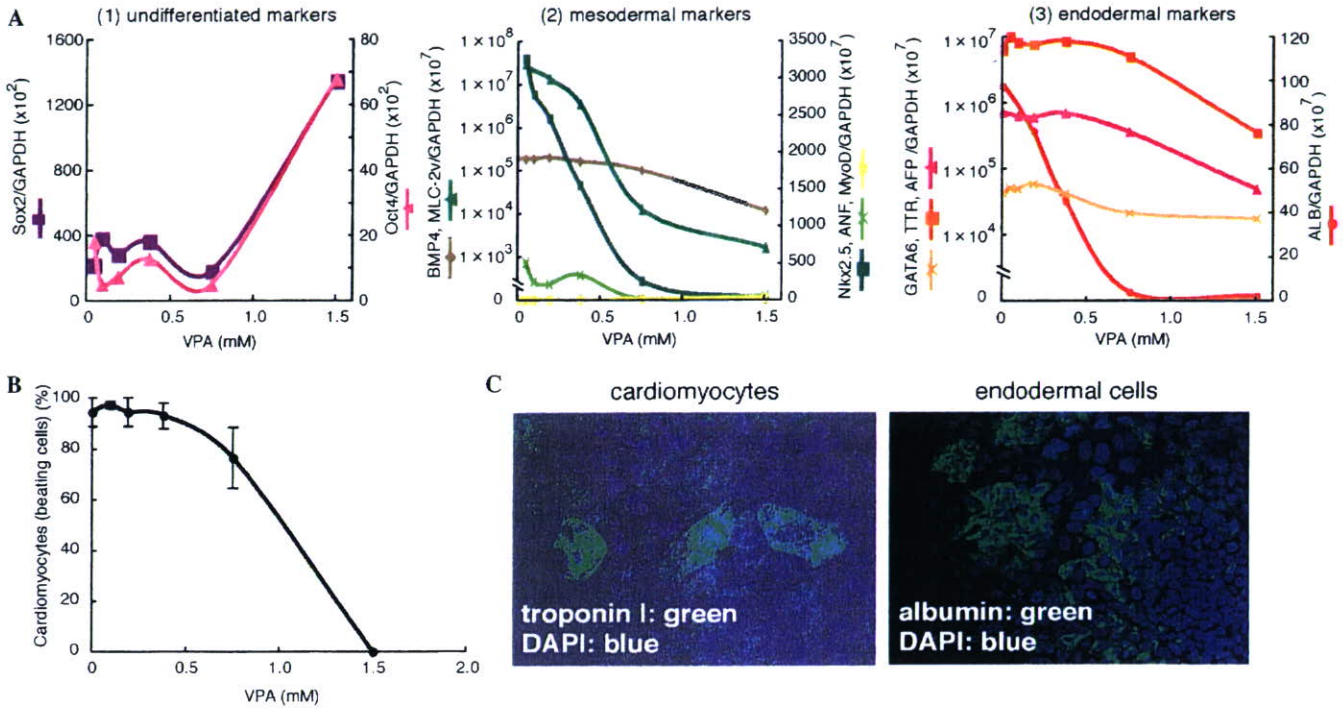

Fig. 2. ES differentiation assay 1: the undifferentiated state and mesodermal and endodermal differentiation. (A) The expression levels of typical undifferentiated markers, Oct4 and Sox2 (1), mesodermal markers, BMP4, MLC-2v, Nkx2.5, ANF, and MyoD (2), and endodermal markers, GATA6, TTR, AFP, and ALB (3), were quantified at each concentration of VPA with real-time RT-PCR. (B) Cardiomyocytes derived from ES cells were analyzed by observing their distinctive beating movements at each concentration of VPA. (C) (left) Cardiomyocytes were immunostained with an anti-troponin I antibody. (right) Endodermal cells derived from ES cells were immunostained with an anti-albumin antibody.

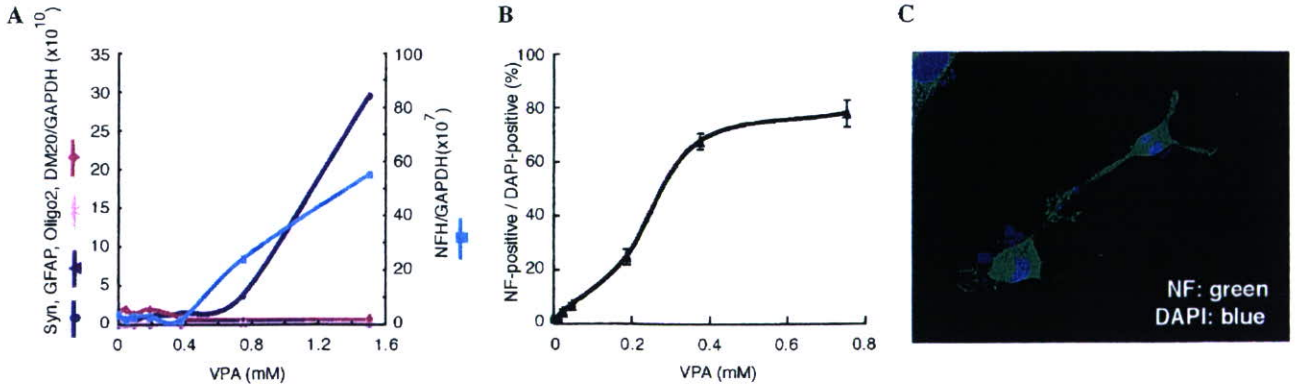

Fig. 3. ES differentiation assay 2: ectodermal differentiation. (A) The expression levels of typical ectodermal markers, Synaptophysin, NFH, GFAP, and Oligo2, were quantified with real-time RT-PCR. (B) The efficiency of neuronal differentiation from ES cells was estimated with anti-neurofilament antibody-stained cells (NF-positive) against total cells (DAPI-positive). (C) Neuronal cells derived from ES cells (VPA 0.38 mM) were immunostained with an anti-neurofilament (NF) 200 antibody.

contractile motions and was shown to decrease in a concentration-dependent manner (Fig. 2B). It was also confirmed that VPA inhibited the differentiation into cardiomyocytes at the molecular and morphological levels. On day 10 of the differentiation assay, a cellular population expressed a definitive endodermal marker, ALB was detected (Fig. 2C, right). The expression levels of GATA6, TTR, AFP, and ALB were decreased in a concentration-dependent manner (Fig. 2A-(3)), suggesting that VPA suppressed the differentiation into endodermal lineages. For ectodermal lineages, the expression levels of neuron-specific markers, such as Synaptophysin (Syn) and NFH, were increased in a concentration-dependent manner. Glial markers, such as GFAP, which is a representative astrocyte-specific marker, and Oligo2 and DM20, which are oligodendrocyte-specific markers, were not induced (Fig. 3A). With a dose of 0.38 mM VPA, many positive cells to neurofilament 200, which is a neuron-specific marker, were detected in samples on day 10 of the differentiation assay (Fig. 3C), and the ratio of anti-neurofilament 200-positive cells was increased in a concentration-dependent manner (Fig. 3B). On the other hand, cells stained with the anti-GFAP antibody were not observed (data not shown). Taken together, these results suggest that VPA promotes ES cells to differentiate into neurons but not glial cells.

Discussion

In the cell viability assay, there was a significant difference in the sensitivities against VPA between ES cells as an embryonic tissue cell model and NIH-3T3 fibroblasts as an adult tissue cell model. VPA has been in clinical use as a safe and effective antiepileptic drug (AED) in a wide range of epileptic conditions in children and adults [12]. Although VPA has been shown to have very few side effects, it is a potent teratogen and produces several malformations in embryos [5,13,14]. Thus, VPA could affect embryonic tissue cells more than adult tissue cells and, consequently, might cause damage to developing cells and, specifically, to embryos. In fact, VPA caused triploblastic differentiations of ES cells in the study herein reported.

Here, we showed that VPA stimulated the differentiation of ES cells into neuronal cells in a lineage-specific manner but attenuated the differentiation of ES cells into endodermal or mesodermal cells. Similarly to this finding in ES cells, VPA is known to promote neuronal fate and to inhibit glial fate simultaneously in multiple adult neural progenitor cells [15]. Whereas VPA can promote the differentiation of the adult neural progenitor cell by induction of neurogenic transcription factors such as NeuroD [15], it remains to be determined what mechanisms of the neuronal differential promotion are involved in ES cells. Nevertheless, it seemed that the altered development of neural cells or tissues driven by VPA could result in NTDs [4], which are predominant VPA-induced teratogenic malformations.

VPA has been reported to inhibit histone deacetylases (HDACs) in a therapeutic range (0.30–0.70 mM) and cause the hyperacetylation of histones in HeLa, F9 teratocarcinoma, and Neuro2A neuroblastoma cells [16,17]. In general, increased levels of histone acetylation are associated with increased transcriptional activity, whereas decreased levels of acetylation are associated with the repression of gene expression [18,19]. A number of specific and potent inhibitors of HDACs, such as trichostatin A (TSA) and VPA, prevent tumorigenesis in rodent and human models and have potential therapeutic roles in the treatment of malignant diseases [20,21]. Furthermore, VPA has been reported to arrest the cell cycle at a G0/1 phase, inhibit proliferation, and induce apoptosis in multiple myeloma [22,23] *in vitro*. Thus, VPA could also inhibit cell proliferation in ES cells by a similar mechanism. In addition, it is also accepted that HDACs play an important role during the embryogenesis of numerous organisms, and interfering with their functions using HDAC inhibitors, such as VPA, could result in some developmental abnormalities, such as teratogenicity [24]. These findings suggest that the effects of VPA on cell growth and neurons might be via the inhibition of HDACs.

Recently, stem cells have become important new tools for the development of *in vitro* model systems to test drugs and chemicals and have shown potential to predict or estimate toxicity [25]. Among various stem cells, ES cells are some of the most valuable cells to develop *in vitro* model systems because they are capable of self-renewing and differentiating into every cell type of the mammalian organism and therefore have higher plasticity than adult stem cells. Since mouse ES cells are prone to differentiate into cardiomyocytes, drug toxicity, such as cardiotoxicity, can be assessed using ES cells [26–30]. The embryonic stem cell test (EST) is an *in vitro* embryotoxicity assay that assesses the ability of chemical compounds to inhibit the differentiation of ES cells into cardiomyocytes [31,32]. In comparison to *in vivo* studies, EST is easy and highly accurate in predicting cellular toxicity, outperforming classical assays, such as fetal limb micromass and post-implantation whole-rat embryo cultures [32]. Thus, EST is a simple and accurate test for toxicity; however, it is not sufficient for evaluating all chemicals because only two parameters of cytotoxicity and morphological change are assessed in the reported EST [8]. Therefore, we attempted to characterize the tissue-specific embryotoxicity of VPA by analyzing the gene expression of the tissue-specific markers as well as by conducting a histological and immunocytochemical study and examining the established two parameters in the mouse embryonic stem (ES) cell differentiation system. Using this system, we demonstrated that VPA is highly cytotoxic and potent to inhibit differentiation into cardiomyocytes in a cytotoxicity and morphological study as well as stimulates the differentiation of the neuronal lineage and inhibits the differentiation of mesodermal and endodermal lineages. Taking the *in vivo* embryotoxicity of VPA into account, the system presented in this study could be useful for predicting the degree of the abnormal neural development of VPA *in vivo*.

In conclusion, this *in vitro* ES cell system allows estimating and characterizing the embryotoxic effects of various chemicals. Further research on this innovative method may help to establish high-throughput screening analysis of drugs to reduce the number of experimental animals and save time.

Acknowledgments

This work was supported in part by research grants from the Scientific Fund of the Ministry of Education, Science, and Culture of Japan, the Ministry of Human Health and Welfare of Japan, and the Japan Health Science.

Appendix A. Supplementary data

Supplementary data associated with this article can be found, in the online version, at doi:10.1016/j.bbrc.2006.10.189.

References

[1] B.F.D. Bourgeois, Valproic Acid—Clinical Efficacy and Use in Epilepsy, in: R.H. Levy, R.H. Mattson, B.S. Meldrum, E. Perucca (Eds.), Antiepileptic Drugs, Lippincot Williams & Wilkins, Philadelphia, 2002, pp. 808–817.

[2] S.D. Silberstein, Clinical Efficacy and Use in Other Neurological Disorders, in: R.H. Levy, R.H. Mattson, B.S. Meldrum, E. Perucca (Eds.), Antiepileptic Drugs, Lippincot Williams & Wilkins, Philadelphia, 2002, pp. 818–827.

[3] H. Nau, R.S. Hauck, K. Ehlers, Valproic acid-induced neural tube defects in mouse and human: aspects of chirality, alternative drug development, pharmacokinetics and possible mechanisms, Pharmacol. Toxicol. 69 (1991) 310–321.

[4] H. Nau, Valproic acid-induced neural tube defects, CIBA Found. Symp. 181 (1994) 144–160.

[5] E.J. Lammer, L.E. Severr, G.P. Oakley Jr., Teratogen update: valproic acid, Teratology 35 (3) (1987) 465–473.

[6] A. Oberemm, F. Kirchbaum, Valproic acid induced abnormal development of the central nervous system of three species of amphibians: implications for neural tube defects and alternative experimental systems, Teratogen. Carcin. Mutagen. 12 (6) (1992) 251–262.

[7] A.I. Whitsel, C.B. Johnson, C.J. Forehand, An *in ovo* chicken model to study the systemic and localized teratogenic effects of valproic acid, Teratology 66 (4) (2002) 153–163.

[8] H. Spielmann, I. Pohl, B. Dröing, M. Liebsch, F. Moldenhauer, The embryonic stem cell test, *in vitro* embryotoxicity test using two permanent mouse cell lines: 3T3 fibroblast and embryonic stem cells, In Vitro Toxicol. 10 (1997) 119–127.

[9] J. Rohwedel, K. Guan, C. Hegert, A.M. Wobus, Embryonic stem cells as an *in vitro* model for mutagenicity, cytotoxicity and embryotoxicity studies: present state and future, Toxicol. In Vitro 15 (2001) 741–753.

[10] A.M. Wobus, K. Guan, H.T. Yang, K. Boheler, Embryonic Stem Cells: Methods and Protocols, in: K. Turksen (Ed.), Methods in Molecular Biology, Humana, Totowa, NJ, 2002, pp. 127–156.

[11] T. Mosman, Rapid colorimetric assay for cellular growth and survival: application to proliferation and cytotoxicity assays, J. Immunol. Methods 65 (1983) 55–63.

[12] E. Lepkifker, I.D.P. Iancu, R. Ziv, M. Kotler, Valproic acid in ultrarapid cycling, Clin. Neuropharmacol. 18 (1995) 72–75.

[13] H. Nau, R. Zierer, H. Spielmann, D. Neubert, C. Gansau, A.H. van Gennip, A new model for embryotoxicity testing: teratogenicity and pharmacokinetics of valproic acid following constant-rate administration in the mouse using human therapeutic drug and metabolite concentrations, Life Sci. 29 (1981) 2803–2814.

[14] K. Wide, B. Winbladh, B. Kallen, Major malformations in infants exposed to antiepileptic drugs in utero, with emphasis on carbamazepine and valproic acid: a nation-wide, population-based register study, Acta Paediatr. 93 (2004) 174–176.

[15] J. Hsieh, K. Nakashima, T. Kuwabara, E. Mejia, F.H. Gage, Histone deacetylase inhibition-mediated neuronal differentiation of multipotent adult neural progenitor cells, Proc. Natl. Acad. Sci. USA 101 (2004) 16659–16664.

[16] R.A. Blaheta, J. Cinatl Jr., Anti-tumor mechanisms of valproate: a novel role for an old drug, Med. Res. Rev. 22 (2002) 492–511.

[17] M. Kaiser, I. Zavrski, J. Sterz, C. Jakob, C. Fleissner, P-M. Kloetzel, O. Sezer, U. Heider, The effects of the Histone deacetylase inhibitor valproic acid on cell cycle, growth suppression and apoptosis in multiple myeloma, Haematologica 91 (2006) 248–251.

[18] M. Gottlicher, S. Minucci, P. Zhu, O.H. Kramer, H.A. Schimpf, S. Giavara, J.P. Sleeman, F. Lo Coco, C. Nervi, P.G. Pelicci, T. Heinzel, Valproic acid defines a novel class of HDAC inhibitors inducing differentiation of transformed cells, EMBO J. 20 (2001) 6969–6978.

[19] C.J. Phiel, F. Zhang, E.Y. Huang, M.G. Guenther, M.A. Lazar, P.S. Klein, Histone deacetylase is a direct target of valproic acid, a potent anticonvulsant, mood stabilizer, and Teratogen, J. Biol. Chem. 276 (2001) 36734–36741.

[20] A.J.M. De Ruijter, A.H. van Gennip, H.N. Caron, S. Kemp, A.B.P. van Kuilenburg, Histone deacetylases (HDACs): characterization of the classical HDAC family, Biochem. J. 370 (2003) 737–749.

[21] R.W. Johnstone, Histone deacetylase inhibitors: novel drugs for the treatment of cancer, Nat. Rev. Drug Discov. 1 (2002) 287–299.

[22] R.J. Lin, T. Sternsdorf, M. Tini, R.M. Evans, Transcriptional regulation in acute promyelocitic leukemia, Oncogene 20 (2001) 7204–7215.

[23] P.P. Pandolfi, Transcriptional therapy for cancer, Oncogene 20 (2001) 3116–3127.

[24] E. Menegola, F. Di Renzo, M.L. Broccia, M. Prudenziati, S. Minucci, V. Massa, E. Giavini, Inhibition of histone deacetylase activity on specific embryonic tissues as anew mechanism for teratogenicity, Birth Defects Res. (part B) 74 (2005) 392–398.

[25] J.C. Davila, G.G. Cezar, M. Thiede, S. Strom, T. Miki, J. Trosko, Use and application of stem cells in toxicology, Toxicol. Sci. 79 (2004) 214–223.

[26] I. Kehat, D. Kenyagin-Karsenti, M. Snir, H. Segev, M. Amit, A.S. Gepstein, E. Livne, O. Binah, J. Itskovitz-Eldor, L. Gepstein, Human embryonic stem cells can differentiate into myocytes with structural and functional properties of cardiomyocytes, J. Clin. Invest. 108 (2001) 407–414.

[27] I. Kehat, A. Gepstein, A. Spira, J. Itskovitz-Eldor, L. Gepstein, High-resolution electrophysiological assessment of human embryonic stem cell-derived cardiomyocytes, Circ. Res. 91 (2002) 659–661.

[28] C. Mummery, D. Ward, C.E. van den Brink, Cardiomyocytes differentiation of mouse and human embryonic stem cells, J. Anat. 200 (2002) 489–493.

[29] D. Choi, H.J. Oh, U.J. Chang, S.K. Koo, J.X. Jiang, S.Y. Hwang, J.D. Lee, G.C. Yeoh, H.S. Shin, J.S. Lee, B. Oh, *In vitro* differentiation of mouse embryonic stem cells into hepatocytes, Cell Transplant. 11 (2002) 359–368.

[30] T. Yamada, M. Yoshikawa, S. Kanda, Y. Kato, Y. Nakajima, S. Ishizaka, Y. Tsunoda, *In vitro* differentiation of embryonic stem cells into hepatocytes-like cells identified by cellular uptake of indocyanine green, Stem Cells 20 (2002) 146–154.

[31] D.R. Newall, K.E. Beedles, The stem cell test: an *in vitro* assay for teratogenic potential. Results of a blind trial with 25 compounds, Toxicol. In Vitro 10 (1996) 229–240.

[32] G. Scholz, E. Genschow, I. Pohl, S. Bremer, M. Apparels, H. Rape, Prevalidation of the embryonic stem cell test EST—a new *in vitro* embryotoxicity test, Toxicol. In Vitro 13 (1999) 675–681.

EXPERIMENTAL CELL RESEARCH 313 (2007) 1886-1896

available at www.sciencedirect.com

ScienceDirect

www.elsevier.com/locate/yexcr

Research Article

Gadd45a, the gene induced by the mood stabilizer valproic acid, regulates neurite outgrowth through JNK and the substrate paxillin in N1E-115 neuroblastoma cells

Junji Yamauchi[a,*], *Yuki Miyamoto*[a], *Mayu Murabe*[a], *Yoko Fujiwara*[a], *Atsushi Sanbe*[a], *Yuko Fujita*[b], *Shoko Murase*[b], *Akito Tanoue*[a]

[a]*Department of Pharmacology, National Research Institute for Child Health and Development 2-10-1 Oukura, Setagaya, Tokyo 157-8535, Japan*

[b]*Biomaster, Inc., Naka, Yokohama 231-0006, Japan*

ARTICLE INFORMATION

Article Chronology:
Received 7 November 2006
Revised version received
12 February 2007
Accepted 15 February 2007
Available online 28 February 2007

Keywords:
VPA
Gadd45a
JNK
Paxillin
Neurite outgrowth

ABSTRACT

Valproic acid (VPA), a mood stabilizer and anticonvulsant, has a variety of neurotrophic functions; however, less is known about how VPA regulates neurite outgrowth. Here, using N1E-115 neuroblastoma cells as the model, we show that VPA upregulates Gadd45a to trigger activation of the downstream JNK cascade controlling neurite outgrowth. VPA induces the phosphorylation of c-Jun N-terminal kinase (JNK) and the substrate paxillin, while VPA induction of neurite outgrowth is inhibited by JNK inhibitors (SP600125 and the small JNK-binding peptide) or a paxillin construct harboring a Ser 178-to-Ala mutation at the JNK phosphorylation. Transfection of Gadd45a, acting through the effector MEKK4, leads to the phosphorylation of the JNK cascade. Conversely, knockdown of Gadd45a with siRNA reduces the effect of VPA. Taken together, these results suggest that upregulation of Gadd45a explains one of the mechanisms whereby VPA induces the neurotrophic effect, providing a new role of Gadd45a in neurite outgrowth.

Introduction

Valproic acid (VPA), which is a compound of the short-chain, branched fatty acid, is a mood-stabilizing agent utilized in the treatment of manic-depressive illness (also known as bipolar disorder) [1,2]. The action mechanism of VPA has been thought to improve the efficiency of neurotransmission through the blockade of neurotransmitter uptake, inhibition of neurotransmitter catabolism, or modulation of neurotransmitter receptors [1,2]. However, increasing evidence has demonstrated that VPA has a variety of neurotrophic effects, such as the enhancement of neurogenesis, protection of neurons, and outgrowth of neurites [1,2]. It is, thus, an important theme to understand the precise mechanism whereby VPA induces neurotrophic effects such as neurite outgrowth.

Mood-stabilizing agents influence multiple signaling pathways underlying neurotrophic factors, such as neurotrophins [2]. One major neurotrophic pathway is linked to the mitogen-activated protein kinase (MAPK)/extracellular-

* *Corresponding author.* Fax: +81 3 5494 7057.
E-mail address: jyamauchi@nch.go.jp (J. Yamauchi).

0014-4827/$ - see front matter © 2007 Elsevier Inc. All rights reserved.
doi:10.1016/j.yexcr.2007.02.019

signal-regulated protein kinase (ERK) signaling cascade [2,3]. This cascade is composed of three conserved components: MAPK kinase kinase (MAPKKK) phosphorylates and activates MAPK kinase (MAPKK), leading to the phosphorylation and activation of MAPK/ERK. A neurotrophic factor binding to the cognate receptor, acting through Ras GTPases and the effector MAPKKKs Raf-1, A-Raf, and B-Raf, induces the activation of ERK. ERK regulates the formation of neurites and survival of neurons by phosphorylating transcription factors and cytoskeletal components [3,4]. It is known that VPA induces neurite outgrowth through ERK and the downstream AP-1 transcriptional complex in SH-SY5Y neuroblastoma cells [5] and primary cortical neurons [6].

Neurotrophic factors also stimulate the signaling cascade of c-Jun N-terminal kinase (JNK), the other subfamily of MAPK [7,8]. Like the ERK cascade, the JNK cascade also consists primarily of three chains of kinase components, while their functions depend on the cell types [9]. It is thus thought that, depending on the developmental stages and cell types, JNK has a positive or negative effect on regulating the cell cycle, differentiation, survival, and cytoskeletal organization. There are many structurally unrelated, upstream regulators of MAPKKKs in the JNK cascade. Gadd45a (also called Gadd45 or Gadd45α) is one such regulator. Gadd45a binds directly to MAPK/ERK kinase kinase 4 (MEKK4), an MAPKKK of the JNK cascade, and activates it [10]. Gadd45a has been originally identified as the gene that is induced by radiation and other stress responses [11]. Therefore, in addition to its simple role as an MAPKKK regulator, Gadd45a is thought to be a multifunctional protein modulating the cell cycle, genomic stability, and stress-related responses in fibroblasts and epithelial cells; however, much less is known about the role of Gadd45a in neuronal cells.

Previously, we reported that JNK and its substrate paxillin mediate serum deprivation-induced neurite extension in N1E-115 neuroblastoma cells [12]. N1E-115 cells show no polarity when neurites outgrow and are, therefore, used as a suitable model to study the early process of neurite outgrowth [13]. In the present study, we show that VPA has the ability to induce neurite outgrowth through a JNK-paxillin unit even in the presence of serum. Furthermore, we have found that Gadd45a is upregulated by VPA and mediates this cascade. The findings provide evidence of the previously uncharacterized role of Gadd45a in neurite outgrowth as well as an answer to how VPA induces neurite outgrowth.

Materials and methods

Materials

The following antibodies were purchased: anti-phosphorylated (pThr^{183}/pTyr^{185}) JNK from Cell Signaling Technology (Beverly, MA); anti-phosphorylated (pSer^{178}) paxillin from Biosource (Camarillo, CA); anti-paxillin from Chemicon (Temecula, CA); anti-JNK, anti-Gadd45a, anti-MEKK4, and anti-HA from Santa Cruz Biotechnology (Santa Cruz, CA); anti-actin from BD Biosciences Pharmingen (Franklin Lake, NJ); anti-FLAG from Sigma Biosciences (St. Louis, MO); and anti-GFP and anti-HA from Medical and Biological Laboratories (Nagoya, Japan). The following chemicals and proteins were purchased: VPA from Wako Pure Chemical Industries (Osaka, Japan); SP600125, JNK inhibitor I, SB203580, *C. difficile* Toxin B, and C3 exoenzyme from Calbiochem–Novabiochem (San Diego, CA); U0126 from Promega (Madison, WI); and collagen (type I) from Sigma Biosciences.

Plasmids

The region encoding paxillinα was amplified by the method of RT-PCR from a mouse brain total RNA. The isolated paxillin was inserted into the jellyfish green fluorescent- and red fluorescent-tagged mammalian expression vectors pEGFP-C1 (Clontech-Takara, Kyoto, Japan) and pJRED-C (Evrogen, Moscow, Russia), respectively. The paxillin construct harboring the Ser 178-to-Ala mutation was produced by the overlapping PCR method and ligated into pEGFP-C1 and pJRED-C. The coding region of Gadd45a was isolated by the RT-PCR method from a total RNA of VPA-stimulated N1E-115 cells and ligated into pEGFP-C1 and pCMV-FLAG [12]. All sequences were confirmed using ABI (Foster City, CA) automatic sequencers. The mammalian expression plasmid encoding HA-JNK1 was kindly provided by Dr. M. Karin (University of California at San Diego, La Jolla, CA).

siRNA preparation

The 21-nucleotide siRNA duplexes were synthesized by Nippon EGT (Toyama, Japan). The siRNA target nucleotide sequences: 5′-AAGACGACGACCGGGATGTGG-3′ (nucleotide number 188–208) for mouse Gadd45a; 5′-AAGTATGGAATCCGATCCAGA-3′ (nucleotide number 165–185) for mouse MEKK4; and 5′-AAGCCATTCTATCCTCTAGAG-3′ for *P. pyralis* luciferase (as the control) were designed according to an online software, siRNA Sequence Selector (http://bioinfo.clontech.com/rnaidesigner/).

Cell culture and transfection

Mouse neuroblastoma N1E-115 cells were cultured in 3.5- to 15-cm cell culture dishes in DMEM containing 10% heat-inactivated FBS, 50 U/ml penicillin, and 50 μg/ml streptomycin at 37 °C in a humidified atmosphere containing 5% CO_2. To keep the ability for differentiation, we selected an N1E-115 cell clone sensitive to normal differentiation following deprivation of serum [13] using the limiting-dilution method. For the experiments, cells were plated on collagen-coated dishes. Unless otherwise indicated, cells were treated with or without 3 mM VPA in the presence or absence of SP600125 (10 μM), JNK inhibitor I (20 μM), U0126 (10 μM), SB203580 (10 μM), *C. difficile* Toxin B (20 ng/ml), or C3 exoenzyme (20 μg/ml) for 48 h. Cells (n=50 to 100) were randomly selected and cells with processes longer than 2 cell bodies were considered to be those bearing neurites. The plasmid encoding a paxillin, Gadd45a, or a JNK construct was transfected into N1E-115 cells using the Lipofectamine Plus reagent (Invitrogen, Carlsbad, CA) according to the manufacturer's protocol. The medium was replaced 4 h after transfection, and cells were cultured in media for 44 additional hours. The transfection efficiency of the plasmid was typically 30% at 48 h post-transfection, using pEGFP-C1 as the control. The siRNAs were transfected into

N1E-115 cells using the Lipofectamine 2000 reagent (Invitrogen) according to the manufacturer's protocol. The medium was replaced 24 h after transfection, and cells were cultured in media for 48 additional hours. The efficiencies of depletion were 98%±1.7% for the Gadd45a siRNA and 97%±2.1% for the MEKK4 siRNA. To confirm the cell viability under these experimental conditions, N1E-115 cells were stained with 0.4% trypan blue. Trypan blue-incorporating cells were fewer than 1% in each experiment. The phase-contrast or fluorescent image was captured using an Eclipse TE-300 microscope system (Nikon, Kawasaki, Japan) with AxioVision 3.1 software (Carl Zeiss, Oberkochen, Germany). The antibodies for Gadd45a and MEKK4 were not available for immunofluorescence (data not shown).

RNA preparation and RT-PCR analysis

Total RNA was prepared by a Trizol (Invitrogen) reagent. The cDNAs were prepared from 1 μg total RNA with Superscript II (Invitrogen) according to the manufacturer's instructions. PCR amplification was carried out at 30 cycles, each cycle consisting of denaturation at 94 °C for 1 min, annealing at 58.5 °C for 1 min, and extension at 72 °C for 0.5 min. The primers used were 5′-CCGGGATCCATGACTTTGGAGGAATTCTCGGCTG-3′ (sense) and 5′-CCGGGATCCTCACCGTTCCGGGAGATTAATCAC-3′ (antisense) for Gadd45a; 5′-CCGGGATCCATGACCCTGGAAGAGCTGGTG-3′(sense) and 5′-CCGGGATCCTCAGCGTTCCTCTAGAGAGATATAGG-3′ (antisense) for Gadd45b; 5′-CCGGGATCCATGACTCTGGAAGAAGTCCGTG-3′ (sense) and 5′-CCGGGATCCTCACTCGGGAAGGGTGATG-3′ (antisense) for Gadd45γ; and 5′-ATGGATGACGATATCGCTGCGCTC-3′ (sense) and 5′-CTAGAAGCATTTGCGGTGCACGATG-3′ (antisense) for β-actin.

Immunoblotting

Cells were lysed in lysis buffer A (50 mM HEPES–NaOH pH 7.5, 20 mM $MgCl_2$, 150 mM NaCl, 1 mM dithiothreitol, 1 mM phenylmethane sulfonylfluoride, 1 μg/ml leupeptin, 1 mM EDTA, 1 mM Na_3VO_4, 10 mM NaF, and 0.5% NP-40) and stored at −80 °C until use, as previously described [12]. After centrifugation, aliquots of the supernatants were subjected into SDS–polyacrylamide gels. The electrophoretically separated proteins were transferred to polyvinylidene difluoride membranes, blocked with Blocking One (Nacalai, Kyoto, Japan), and immunoblotted with primary antibodies. The bound antibodies were detected using the ECL or ECL-Plus system (Invitrogen) with secondary, anti-rabbit or anti-mouse IgG antibodies conjugated with horseradish peroxidase according to the manufacturer's protocol. Three to five separate experiments were carried out. The band intensity in each immunoblot was semi-quantified using gel-digitizing software. The levels of the phosphorylated forms were normalized to the amount of total kinase. A representative experiment is shown in the figure.

Statistical analysis

The values shown represent the mean±S.D. from separate experiments. ANOVA was followed by Fisher's PLSD (protected least significant difference) post hoc comparisons (*, $p<0.01$; **, $p<0.05$).

Results

VPA induces neurite outgrowth in N1E-115 cells

To explore the signaling mechanism(s) whereby neurites outgrow, we screened available chemical compounds including inhibitors and pharmacological reagents using N1E-115 cells as a neuronal model. N1E-115 cells proliferate in the presence of serum and differentiate by serum deprivation [13], as seen in other neuroblastoma cell lines. The mood stabilizer VPA was one of the compounds that had a potent effect on inducing neurite outgrowth, even in the presence of serum. Cells strikingly began to extend neurites at 24 h after stimulation with VPA. Approximately 40% of cells displayed a phenotype with long neurites at 48 h, and the effect of VPA nearly reached a maximal response at 3 mM (Figs. 1A and B). Since VPA is known to have activity as an inhibitor of histone deacetylase (HDAC) and is able to effectively inhibit cellular HADC activities at the concentration of 3 mM [14,15], we examined whether trichostatin A [16], a specific inhibitor of HDAC, induces neurite outgrowth. Treatment with trichostatin A did not show a significant effect at the concentration of 10–300 nM within at least 48 h (Fig. 1C). It is unlikely that the inhibition of HDAC directly affects neurite outgrowth. We further checked the effect of roscovitine [17], an inhibitor of cyclin-dependent kinases, but it did not cause neurite outgrowth at the concentration of 1–30 μM (Fig. 1D), suggesting that inhibition of the cell cycle is insufficient for neurite outgrowth. These results raised the possibility that VPA might regulate neurite outgrowth through signal network(s) that had so far not been reported as the signaling pathway regulated by VPA.

JNK plays a key role in VPA-induced neurite outgrowth

We previously reported that JNK participates in serum-deprivation-induced neurite extension in N1E-115 cells [12]. Therefore, we investigated whether SP600125, a JNK inhibitor, affects neurite outgrowth induced by VPA. As shown in Figs. 1E and F, the effect of VPA was blocked by SP600125. Since SP600125 is likely to have wider specificity than initially expected [18], we used a more specific inhibitor, JNK inhibitor I [19], which is structurally unrelated to SP600125. JNK inhibitor I is engineered by linking the 20 amino acids of the JNK inhibitory domain of the JNK scaffold protein JIP1 to the HIV-TAT sequence. This inhibitor also had an inhibitory effect on neurite outgrowth, consistently with the result of SP600125. In addition, U0126, a specific inhibitor of the ERK cascade, inhibited the outgrowth by more than 50% (Fig. 1G). In contrast, SB203580, a p38 MAPK inhibitor, did not have obvious effects on the outgrowth (Fig. 1H). These results suggest that JNK, as well as ERK [5,6], is required for VPA-induced neurite outgrowth.

Next, we examined whether JNK is activated following stimulation with VPA. We performed an immunoblot with an

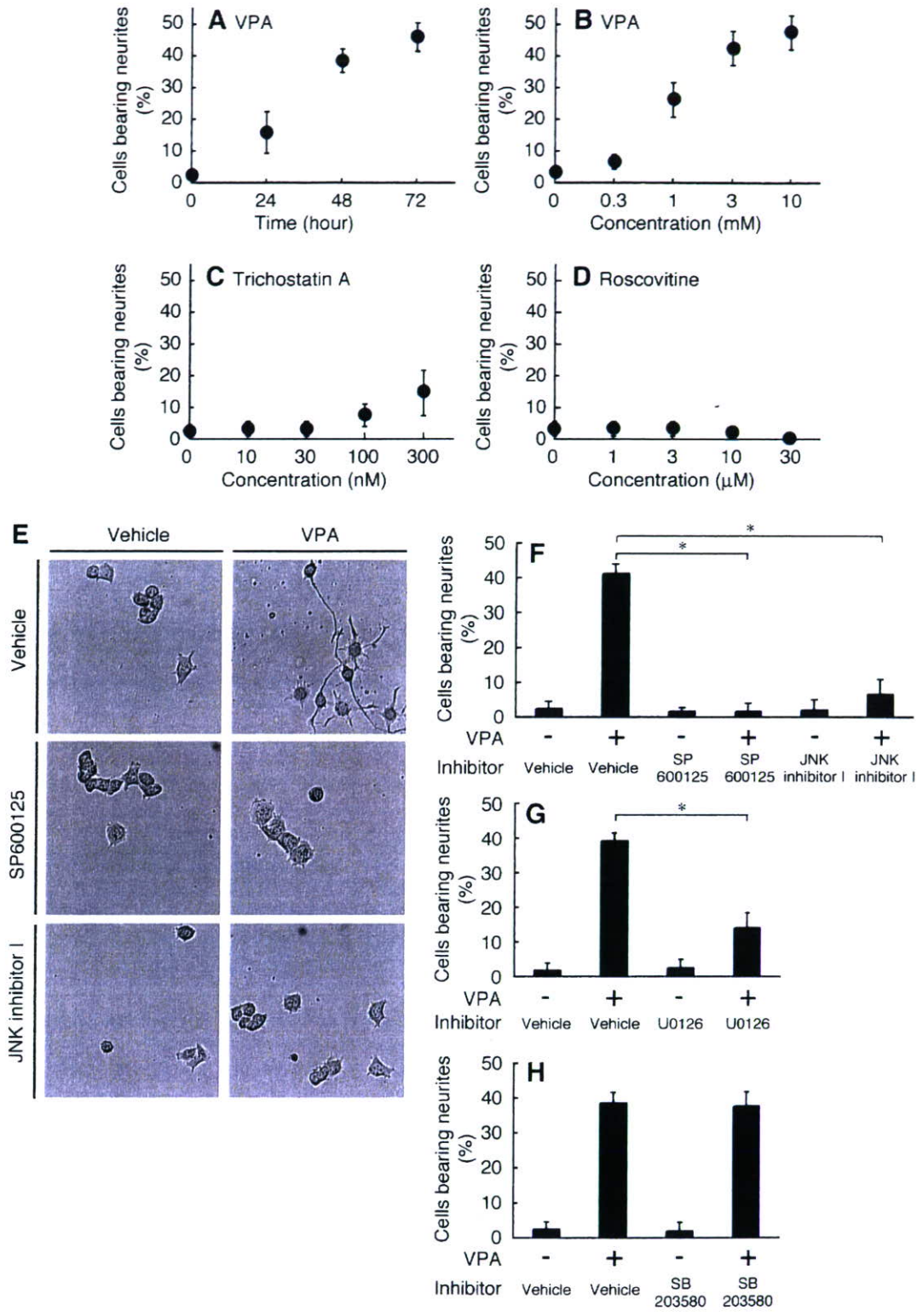

Fig. 1 – VPA induces neurite outgrowth through JNK, as well as ERK, in N1E-115 cells. N1E-115 cells were treated with 3 mM VPA for 0 to 72 h (A) or with the indicated concentration of VPA (B), trichostatin A (C), or roscovitine (D) for 48 h. Cells were incubated with or without 3 mM VPA in the presence or absence of SP600125 or JNK inhibitor I (E, F) U0126 (G), or SB203580 (H) and allowed to extend processes for 48 h. Data were evaluated using one-way ANOVA (*, $p<0.01$).

anti-phosphorylated JNK antibody, which recognizes the active state [9]. JNK was phosphorylated in a time-dependent manner, and the level of phosphorylation reached maximum at 36 h after VPA stimulation (Figs. 2A and B), suggesting that JNK may be an essential component to control neurite outgrowth in N1E-115 cells.

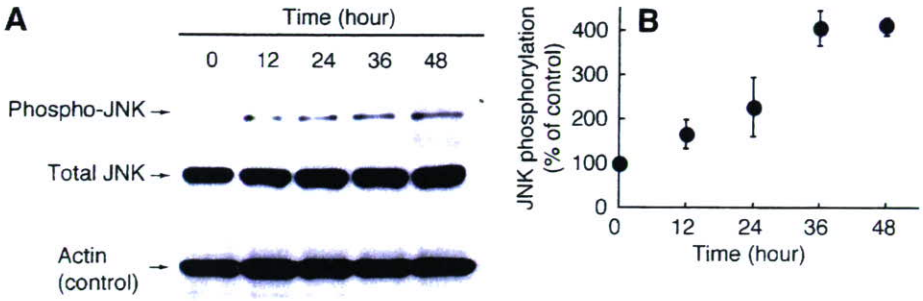

Fig. 2 – JNK is phosphorylated following stimulation with VPA. (A) After the addition of VPA, the lysates of cells were immunoblotted with an anti-phosphorylated JNK antibody. Total JNK was detected using an anti-JNK antibody. The expression of actin is also shown. (B) The band intensity in the immunoblot was semi-quantified. The levels of phosphorylated forms were normalized to the amount of total kinase.

JNK phosphorylation of paxillin mediates VPA-induced neurite outgrowth

A focal adhesion protein paxillin is phosphorylated at Ser 178 by JNK to regulate the migration of fish keratinocytes and rat bladder tumor epithelial NBT-II cells [20,21] and to mediate serum-deprivation-induced neurite extension in N1E-115 cells [12]. We, thus, asked whether the JNK substrate paxillin is required for neurite outgrowth induced by VPA. Transfection of a paxillin construct harboring a Ser 178-to-Ala mutation at the JNK phosphorylation inhibited neurite outgrowth by VPA, while wild-type paxillin

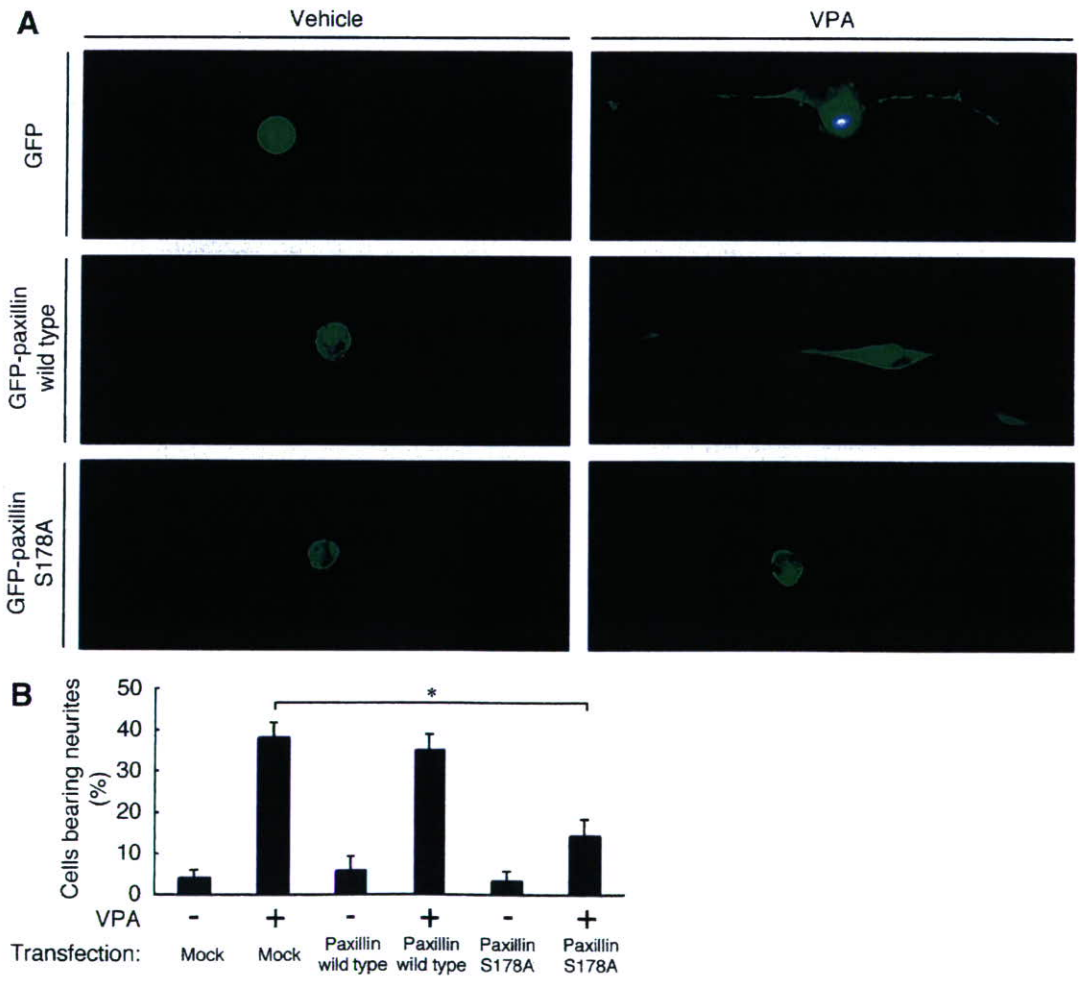

Fig. 3 – JNK phosphorylation of paxillin mediates VPA-induced neurite outgrowth. (A, B) Cells were transfected with the plasmid encoding GFP or GFP-paxillin (wild-type or S178A). The transfected cells were treated with or without VPA and allowed to extend processes for 48 h. Data were evaluated using one-way ANOVA (*, $p<0.01$).

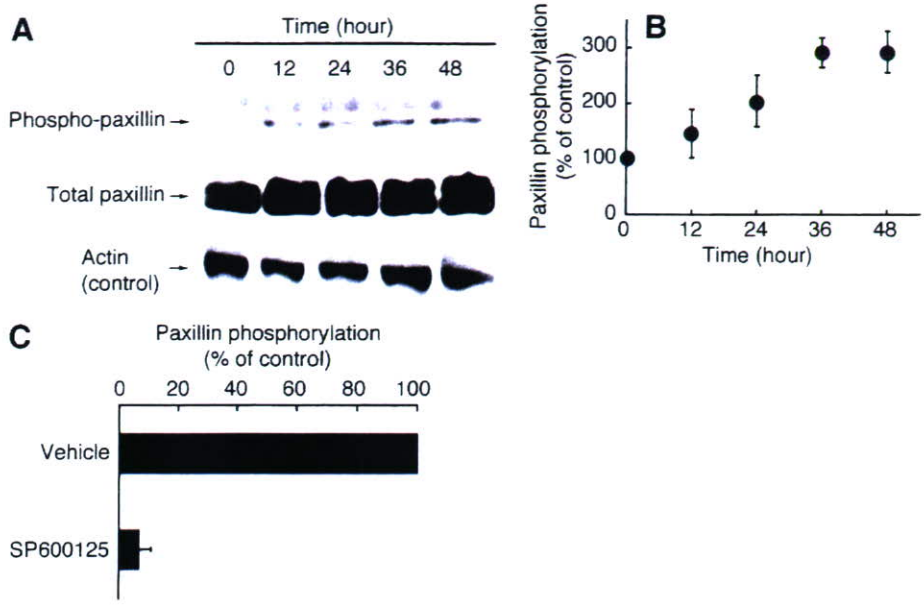

Fig. 4 – VPA stimulates the phosphorylation of paxillin at Ser 178. (A) After the addition of VPA, the lysates of cells were immunoblotted with an anti-phosphorylated paxillin antibody. Total paxillin was detected using an anti-paxillin antibody. The expression of actin is also shown. (B) The levels of the phosphorylated forms of paxillin in the immunoblot were semi-quantified using gel-digitizing software. (C) Cells were incubated with VPA for 48 h in the presence or absence of SP600125.

did not have a significant effect on the outgrowth (Figs. 3A and B). These findings suggest the importance of the phosphorylation of paxillin by JNK in VPA-induced neurite outgrowth.

To confirm that VPA actually stimulates the phosphorylation of paxillin at Ser 178, we carried out an immunoblot using an anti-phosphorylated paxillin antibody. Stimulation with VPA induced phosphorylation of paxillin in a time-dependent manner, and the level of phosphorylation reached the maximum at 36 h (Figs. 4A and B), as observed in the time course of JNK. In addition, SP600125 blocked the phosphorylation of paxillin (Fig. 4C), indicating that stimulation with VPA leads to neurite outgrowth through JNK and the substrate paxillin.

Role of Gadd45, the gene upregulated by VPA, as the regulator of neurite outgrowth in N1E-115 cells

Rac1 and Cdc42 act upstream of JNK in the process of N1E-115 cell differentiation [12]. Pretreatment of *C. difficile* Toxin B, which glycosylates and inhibits RhoA, Rac1, and Cdc42, only partially inhibited neurite outgrowth by VPA (Fig. 5). In addition, the C3 exoenzyme, which ADP-ribosylates RhoA to block its function, did not show an obvious effect. We, thus, searched for a regulator upstream of JNK and paxillin by comparing public bioinformatics databases, such as KEGG (http://www.genome.ad.jp/kegg/), with our Affimetrix Genechip's data (0 versus 48 h after stimulation with 3 mM VPA). Gadd45a was one such candidate gene upregulated by VPA. Importantly, Gadd45a is a direct activator of MEKK4, the MAPKKK of the JNK cascade [10]. However, as far as we could ascertain, there was no information concerning the relationships between Gadd45a and neurite behavior. As shown in Figs. 6A and B, Gadd45a was clearly upregulated by stimulation with VPA in the levels of RNA and protein, while two other Gadd45 family genes (Gadd45b and Gadd45γ) were not changeable.

Next, we tested the possibility that VPA regulates neurite outgrowth through Gadd45a. We transfected a Gadd45a siRNA oligonucleotide to knockdown endogenous Gadd45a expression. The expression of Gadd45a was markedly downregulated by transfection with Gadd45a siRNA, whereas the expression of the control actin was unaffected, as revealed by immunoblotting (Fig. 6C). Knockdown of Gadd45a reduced neurite outgrowth (Fig. 6D). Conversely, transfection with the plasmid encoding Gadd45a enhanced neurite outgrowth (Figs. 6E and F). These results implicated the role of Gadd45a, the gene upregulated by VPA, in neurite outgrowth.

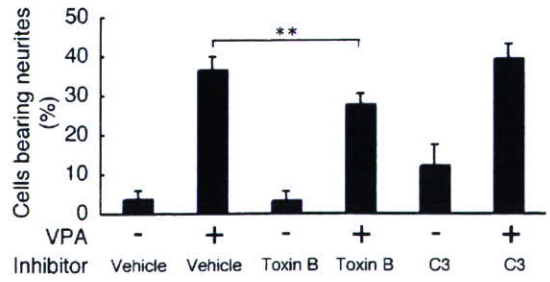

Fig. 5 – Neurite outgrowth by VPA only partially depends on Rho GTPases. Cells were treated with or without VPA in the presence or absence of *C. difficile* Toxin B or C3 exoenzyme and allowed to extend processes for 48 h. Data were evaluated using one-way ANOVA (, $p<0.05$).**

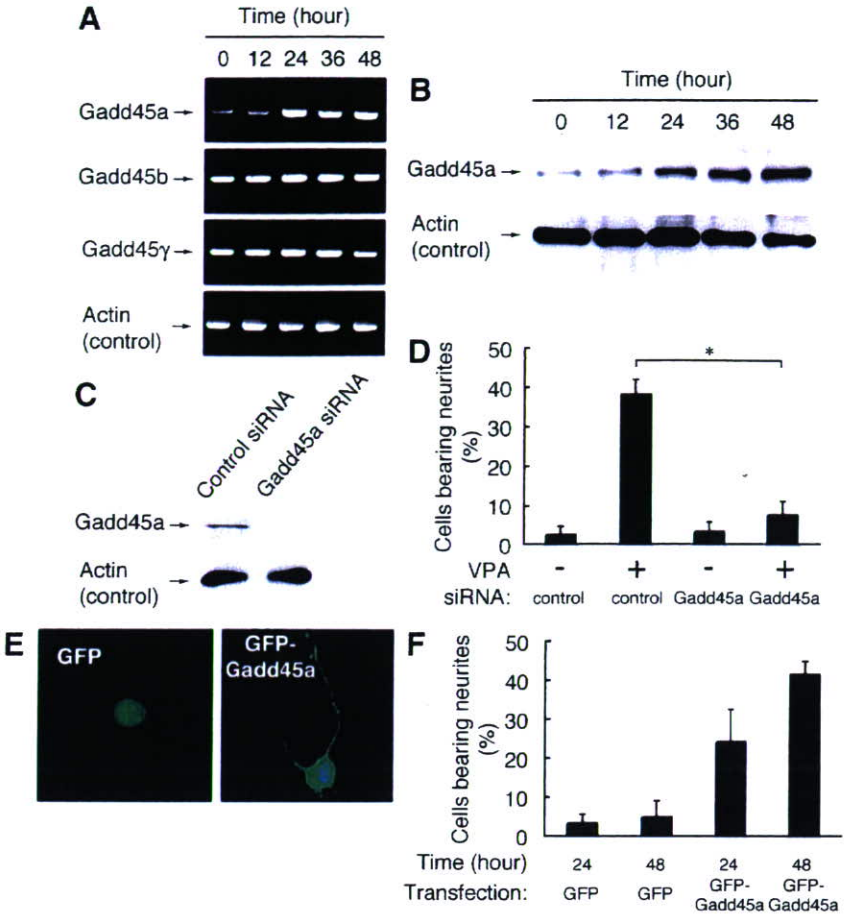

Fig. 6 – VPA upregulates Gadd45a to induce neurite outgrowth in N1E-115 cells. The levels of Gadd45a were analyzed using the methods of RT-PCR (A) and immmunoblotting with an anti-Gadd45a antibody (B). Actin is shown as the control. (C) Cells were transfected with control or Gadd45a siRNA. To confirm the effect of Gadd45a siRNA, the lysates from transfected cells were immunoblotted with an anti-Gadd45a or anti-actin antibody. (D) Transfected cells were incubated with or without VPA and allowed to extend processes. (E, F) Cells were transfected with the plasmid encoding GFP or GFP-Gadd45a and allowed to extend processes for the indicated time. Data were evaluated using one-way ANOVA (*, $p<0.01$).

Gadd45a acts upstream of JNK and paxillin

We investigated whether Gadd45a induces neurite outgrowth through JNK and the substrate paxillin. SP600125 blocked neurite outgrowth induced by Gadd45a (Fig. 7A). In contrast, U0126 did not affect it (Fig. 7B). It is likely that Gadd45a specifically mediates the outgrowth through JNK but not through ERK. In addition, the outgrowth induced by expression of GFP-tagged Gadd45a was inhibited by coexpression of JRED-tagged paxillin harboring a Ser 178-to-Ala mutation (Figs. 7C and D). Furthermore, the phosphorylation of JNK and paxillin was stimulated by the transfection of Gadd45a (Figs. 8A and B), suggesting that Gadd45a acts upstream of the JNK cascade.

Gadd45a activates JNK through MEKK4

Takekawa and Saito [10] demonstrated that Gadd45 family proteins bind to the regulatory domain of MEKK4 and directly activate it. In order to confirm that MEKK4 is involved in the signaling pathway coupling Gadd45a to the phosphorylation of paxillin, we used an MEKK4 siRNA oligonucleotide. The expression of MEKK4 was markedly downregulated by transfection with MEKK4 siRNA, whereas the expression of control actin was unaffected (Fig. 9A). Transfection with MEKK4 siRNA decreased neurite outgrowth induced by Gadd45a as well as VPA (Figs. 9B and C). Similarly, knocking down MEKK4 inhibited the phosphorylation of JNK and paxillin by VPA or Gadd45a (Figs. 10A–D). These results collectively suggest that Gadd45a, acting through MEKK4, triggers the signal leading to neurite outgrowth.

Discussion

Mood-stabilizing agents affect multiple signaling pathways, one of which involves ERK [5,6]. Many neurotrophic factors, acting through ERK and the substrates, such as transcription factors and cytoskeletal proteins, produce cellular neurotrophic actions including neurogenesis, survival, neurite outgrowth, and/or regeneration [3]. In addition to the ERK

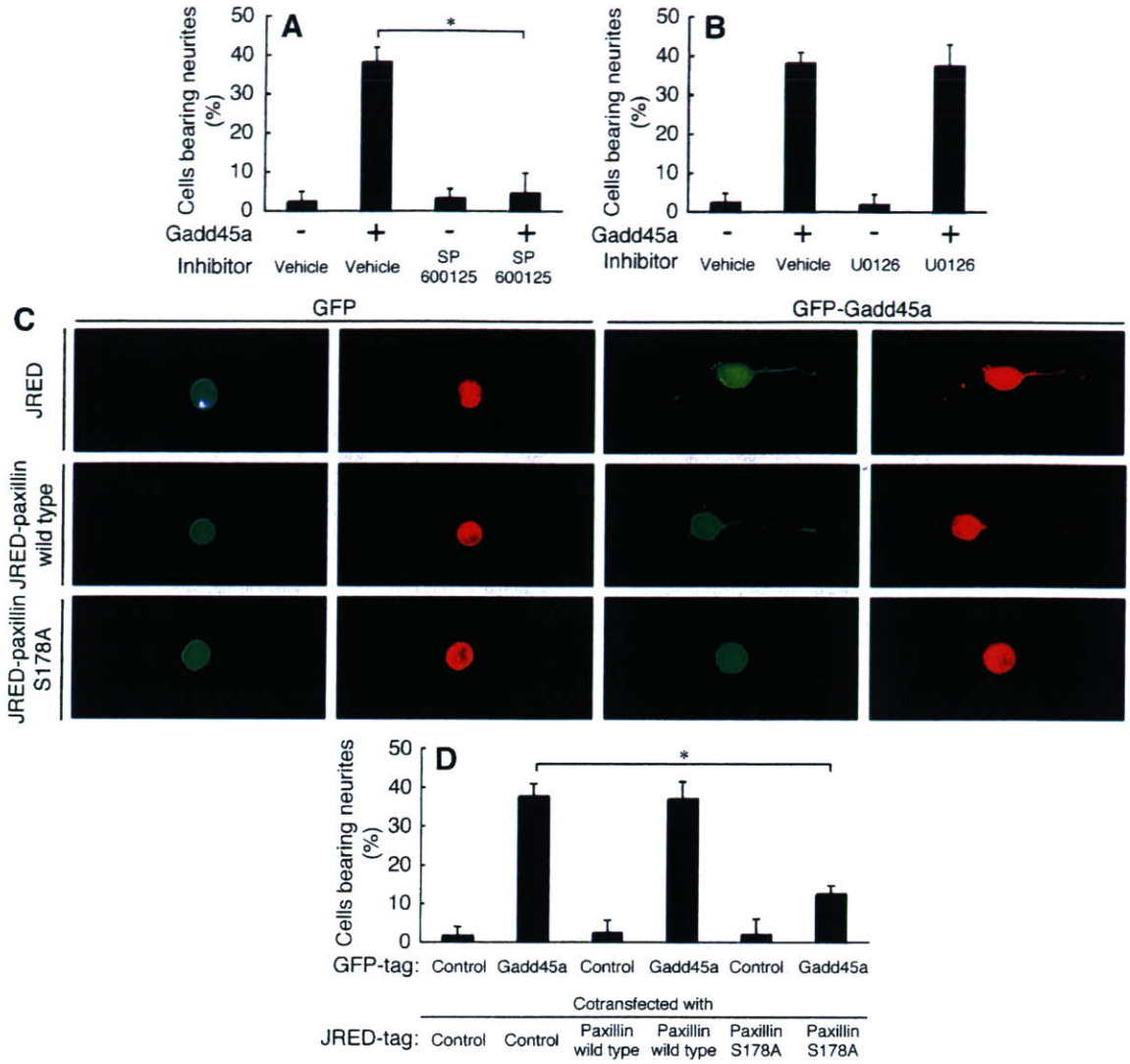

Fig. 7 – Gadd45a induces neurite outgrowth through JNK and paxillin. Cells transfected with the plasmid encoding GFP or GFP-Gadd45a were allowed to extend processes in the presence or absence of SP600125 (A) or U0126 (B). (C, D) Cells were cotransfected with the plasmid encoding GFP or GFP-Gadd45a together with JRED or JRED-paxillin (wild-type or S178A). Data were evaluated using one-way ANOVA (*, $p<0.01$).

signaling pathway, we show here that the mood stabilizer VPA induces neurite outgrowth through the activation of JNK and the phosphorylation of the focal adhesion protein paxillin in N1E-115 cells even in the presence of serum. This conclusion is supported by the findings that JNK inhibitors SP600125 and TAT-JBD or a paxillin construct harboring a Ser 178-to-Ala mutation at the JNK phosphorylation site inhibits neurite outgrowth by VPA and that VPA induces the phosphorylation of JNK and paxillin. Importantly, VPA upregulates Gadd45a, which, through the effector MEKK4, activates the downstream JNK cascade to induce neurite outgrowth. VPA, thus, causes neurites to outgrow by activating at least two types of MAPKs JNK and ERK [5,6], although Gadd45a is the upstream regulator for JNK alone and not for ERK. We previously reported that serum-deprivation-induced neurite extension involves the phosphorylation of JNK and paxillin [12]. While the JNK phosphorylation of paxillin is a common event in both VPA- and serum-deprivation-induced neurite outgrowth, their upstream regulators seem likely to be different. Gadd45a was also upregulated in serum-deprivation-induced neurite outgrowth but the knockdown of Gadd45a had only a partial inhibitory effect on JNK activation and neurite outgrowth (data not shown). It would be interesting to determine which step is a precise convergent point in the signaling pathways underlying VPA- and serum-deprivation-induced neurite outgrowth.

A knockout study of Gadd45a suggests its role as a trigger to modulate certain cellular processes only after cellular injury [22]. Besides such an originally discovered role in cell cycle arrest, recent findings indicate that Gadd45a and two other Gadd45 family proteins, acting through various binding proteins, participate not only in regulating the cell cycle negatively but also in controlling intracellular signaling pathways positively [10,23]. Indeed, N1E-115 cell differentiation can require the suppression of a cell cycle, but it is unlikely that only the suppression is sufficient for the differentiation. In fact, a cell cycle inhibitor in N1E-115 cells did not have an

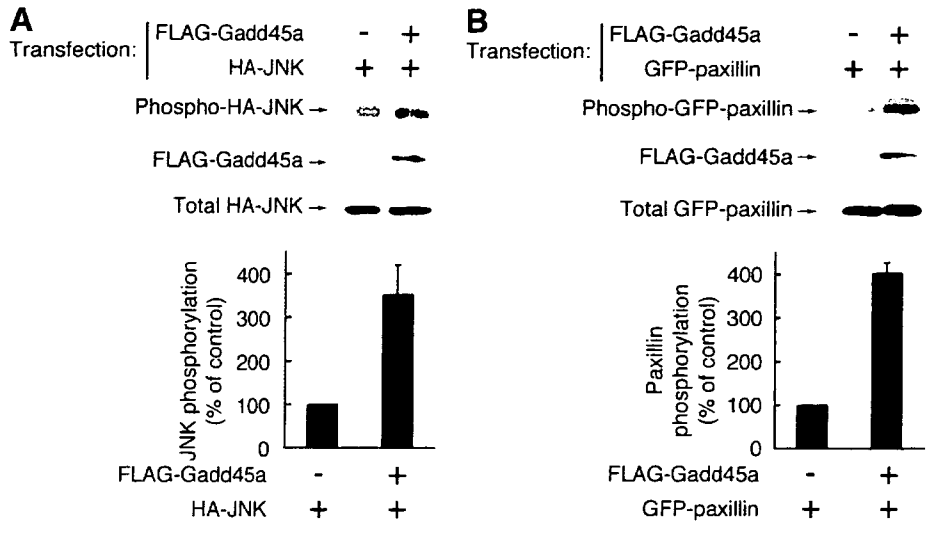

Fig. 8 – Gadd45a stimulates the phosphorylation of JNK and the substrate paxillin. Cells were transfected with the plasmid encoding mock or FLAG-Gadd45a with HA-JNK or GFP-paxillin. The lysates from transfected cells were immunoblotted with an anti-phosphorylated JNK (A) or anti-phosphorylated paxillin (B) antibody. The band intensity in the immunoblot was semi-quantified.

obvious effect on inducing neurite outgrowth under our experimental conditions. In addition, JNK, acting through a Gadd45a-binding partner MEKK4, plays a key role in the VPA-induced neurite outgrowth of N1E-115 cells. In contrast, studies on Gadd45a–/– MEF cells show that, under genomic injury such as UV radiation, the JNK signal has no relationship with the Gadd45a signal [24]. These findings suggest that Gadd45a can use different effector pathways depending on the upstream signal and/or cell type.

Increasing evidence indicates that JNK and the regulators are required for the development of neuronal tissues. Mice doubly lacking JNK1 and JNK2 show neural tube defects [25,26]. Similarly, MEKK4–/– embryos significantly exhibit neural tube defects [27], as seen in knockin embryos homozygous for kinase-inactive MEKK4 K1361R [28]. More importantly, Gadd45-deficient embryos also display the defects [22,23]. Although the abnormality observed among embryos deficient in Gadd45a, MEKK4, or JNK1/2 partially differs or overlaps, the Gadd45a-MEKK4-JNK signaling unit likely plays a key role in the formation of the neural tube *in vivo*. It is, thus, possible that VPA gives rise to neurotrophic functions by regulating the Gadd45a-MEKK4-JNK unit *in vivo*.

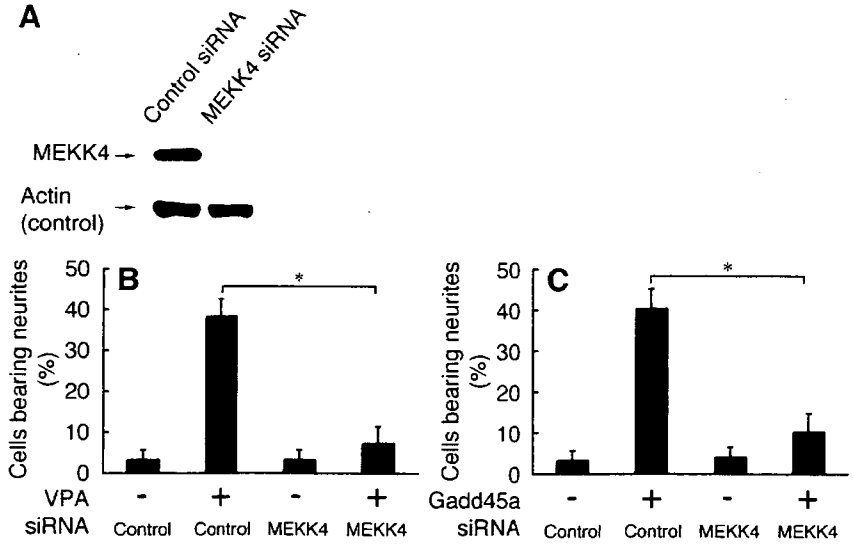

Fig. 9 – Involvement of MEKK4, a binding partner of Gadd45a, in VPA- or Gadd45a-induced neurite outgrowth. Cells were transfected with control or MEKK4 siRNA. (A) To confirm the effect of MEKK4 siRNA, the lysates from transfected cells were immunoblotted with an anti-MEKK4 or anti-actin antibody. (B, C) The effect of MEKK4 siRNA on VPA- or Gadd45a-induced neurite outgrowth was examined. Data were evaluated using one-way ANOVA (*, $p<0.01$).

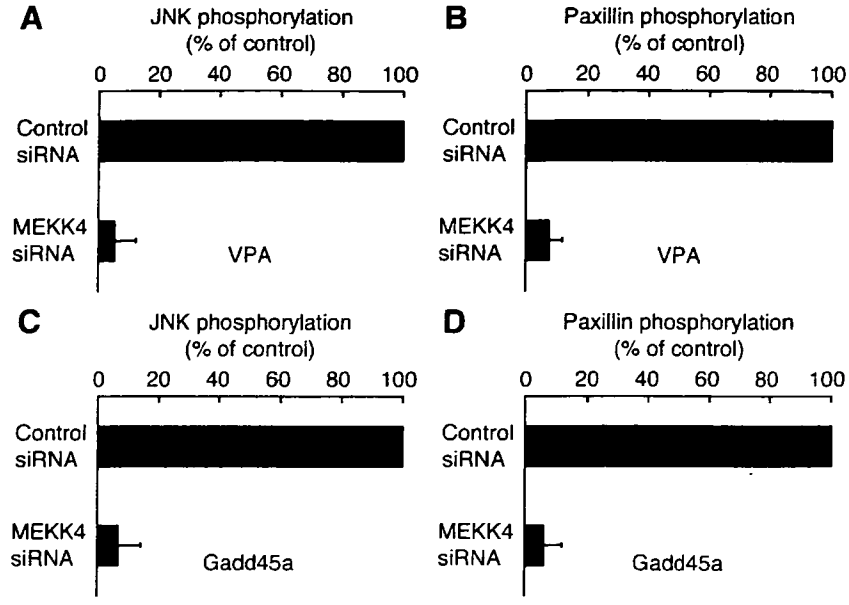

Fig. 10 – VPA or Gadd45a stimulates the phosphorylation of JNK and the substrate paxillin through MEKK4. (A, B) Phosphorylation of JNK or paxillin by VPA was inhibited with transfection with MEKK4 siRNA. (C, D) MEKK4 siRNA also reduced the phosphorylation of JNK or paxillin induced by Gadd45a.

Paxillin is a focal adhesion protein linking extracellular matrix receptors, such as integrins, to the actin cytoskeleton and is phosphorylated at many sites in a signal-dependent manner [21]. Paxillin contains two major phosphorylation sites, tyrosine residues 31 and 118, but these sites are not essential for the neurite outgrowth of pheocromocytoma (PC) 12 cells [29]. Recent biochemical and bioinformatic studies show that paxillin is phosphorylated by an MAPK family other than JNK [21,30]. The phosphorylation of paxillin at Ser 83 by p38 MAPK is involved in nerve growth factor (NGF)-induced neurite outgrowth [31]; however, it is unlikely that p38 MAPK has a positive role in VPA-induced neurite outgrowth since the p38 MAPK inhibitor SB203580 did not effectively block the outgrowth. Paxillin contains some ERK phosphorylation sites. Among them, the phosphorylation at Ser 130 is important for NGF-induced neurite outgrowth [32]. This phosphorylation by ERK is required to induce second phosphorylation at Ser 126 by glycogen synthase kinase (GSK) 3 [32]. Since U0126, the ERK pathway inhibitor, has an inhibitory effect on VPA-induced neurite outgrowth, it is conceivable that the sequentially phosphorylating mechanism through ERK and GSK3 may participate in the VPA-dependent outgrowth.

Using well-established pharmacological reagents and molecular biology tools, we have identified Gadd45a as the new gene upregulated by the mood stabilizer VPA and the downstream JNK cascade as the inducer of neurite outgrowth in N1E-115 cells. These findings have revealed an unexpected role of Gadd45a in neurite outgrowth. Further study on the detailed mechanism underlying neurite outgrowth by VPA is necessary to promote our understanding of not only how VPA upregulates Gadd45a but also whether Gadd45a acts as the regulator of the outgrowth in primary neurons. Such studies could allow for clarifying the exact action point(s) of VPA and help to develop further therapeutic strategies for manic-depressive illness.

Acknowledgments

We thank Drs. E. M. Shooter and Y. Kaziro for their participation in insightful discussions and for providing encouragement. We also thank Drs. J. R. Chan, K. Ide, and D. Shiokawa for their participation in helpful discussions. This work was supported by Grants-in-Aid for Scientific Research from the Ministry of Education, Culture, Sports, Science, and Technology and the Ministry of Health, Labor, and Welfare and partially by grants from the Astellas Metabolic Disease Foundation, the Human Science Foundation, the Kampo Science Foundation, the Kowa Life Science Foundation, the Nakajima Foundation, the Samuro Kakiuchi Memorial Foundation, and the Uehara Memorial Foundation.

REFERENCES

[1] H.K. Manji, W.C. Drevets, D.S. Charney, The cellular neurobiology of depression, Nat. Med. 7 (2001) 541–547.
[2] J.T. Coyle, R.S. Duman, Finding the intracellular signaling pathways affected by mood disorder treatments, Neuron 38 (2003) 157–160.
[3] E.J. Huang, L.F. Reichardt, Neurotrophins: roles in neuronal development and function, Annu. Rev. Neurosci. 24 (2001) 677–736.
[4] D. Bar-Sagi, A. Hall, Ras and Rho GTPases: a family reunion, Cell 103 (2000) 227–238.
[5] P.X. Yuan, L.D. Huang, Y.M. Jiang, J.S. Gutkind, H.K. Manji, G. Chen, The mood stabilizer valproic acid activates mitogen-activated protein kinases and promotes neurite growth, J. Biol. Chem. 276 (2001) 31678–31683.
[6] H. Einat, P.X. Yuan, T.D. Gould, J. Li, J. Du, L. Zhang, H.K. Manji, G. Chen, The role of the extracellular signal-regulated kinase signaling pathway in mood modulation, J. Neurosci. 23 (2004) 7311–7316.

[7] J. Yamauchi, J.R. Chan, E.M. Shooter, Neurotrophin 3 activation of TrkC induces Schwann cell migration through the c-Jun N-terminal kinase pathway, Proc. Natl. Acad. Sci. U. S. A. 100 (2003) 14421–14426.
[8] J. Yamauchi, J.R. Chan, Y. Miyamoto, G. Tsujimoto, E.M. Shooter, The neurotrophin-3 receptor TrkC directly phosphorylates and activates the nucleotide exchange factor Dbs to enhance Schwann cell migration, Proc. Natl. Acad. Sci. U. S. A. 102 (2005) 5198–5203.
[9] R.J. Davis, Signal transduction by the JNK group of MAP kinases, Cell 103 (2000) 239–252.
[10] M. Takekawa, H. Saito, A family of stress-inducible GADD45-like proteins mediates activation of the stress-responsive MTK1/MEKK4 MAPKKK, Cell 95 (1998) 521–530.
[11] A.J. Fornace Jr., I. Alamo Jr., M.C. Hollander, DNA damage-inducible transcripts in mammalian cells, Proc. Natl. Acad. Sci. U. S. A. 85 (1988) 8800–8804.
[12] J. Yamauchi, Y. Miyamoto, A. Sanbe, A. Tanoue, JNK phosphorylation of paxillin, acting through the Rac1 and Cdc42 signaling cascade, mediates neurite extension in N1E-115 cells, Exp. Cell Res. 312 (2006) 2954–2961.
[13] M. Hirose, T. Ishizaki, N. Watanabe, M. Uehata, O. Kranenburg, W.H. Moolenaar, F. Matsumura, M. Maekawa, H. Bito, S. Narumiya, Molecular dissection of the Rho-associated protein kinase (p160ROCK)-regulated neurite remodeling in neuroblastoma N1E-115 cells, J. Cell Biol. 141 (1998) 1625–1636.
[14] M. Gottlicher, S. Minucci, P. Zhu, O.H. Kramer, A. Schimpf, S. Giavara, J.P. Sleeman, F. Lo Coco, C. Nervi, P.G. Pelicci, T. Heinzel, Valproic acid defines a novel class of HDAC inhibitors inducing differentiation of transformed cells, EMBO J. 20 (2001) 6969–6978.
[15] C.J. Phiel, F. Zhang, E.Y. Huang, M.G. Guenther, M.A. Lazar, P.S. Klein, Histone deacetylase is a direct target of valproic acid, a potent anticonvulsant, mood stabilizer, and teratogen, J. Biol. Chem. 276 (2001) 36734–36741.
[16] M. Yoshida, M. Kijima, M. Akita, T. Beppu, Potent and specific inhibition of mammalian histone deacetylase both in vivo and in vitro by trichostatin A, J. Biol. Chem. 265 (1990) 17174–17179.
[17] N. Gray, L. Detivaud, C. Doerig, L. Meijer, ATP-site directed inhibitors of cyclin-dependent kinases, Curr. Med. Chem. 6 (1999) 859–875.
[18] J. Bain, H. McLauchlan, M. Elliott, P. Cohen, The specificities of protein kinase inhibitors: an update, Biochem. J. 371 (Part 1) (2003) 199–204.
[19] C. Bonny, A. Oberson, S. Negri, C. Sauser, D.F. Schorderet, Cell-permeable peptide inhibitors of JNK, Diabetes 50 (2001) 77–82.
[20] C. Huang, Z. Rajfur, C.H. Borchers, M.D. Schaller, K. Jacobson, JNK phosphorylates paxillin and regulates cell migration, Nature 424 (2003) 219–223.
[21] M.C. Brown, C.E. Turner, Paxillin: adapting to change, Physiol. Rev. 84 (2004) 1315–1339.
[22] M.C. Hollander, M.S. Sheikh, D.V. Bulavin, K. Lundgren, L. Augeri-Henmueller, R. Shehee, T.A. Molinaro, K.E. Kim, E. Tolosa, J.D. Ashwell, M.P. Rosenberg, Q. Zhan, P.M. Fernandez-Salguero, W.F. Morgan, C.X. Deng, A.J. Fornace Jr., Genomic instability in Gadd45a-deficient mice, Nat. Genet. 23 (1999) 176–184.
[23] D.M. Juriloff, M.J. Harris, Mouse models for neural tube closure defects, Hum. Mol. Genet. 9 (2000) 993–1000.
[24] X. Wang, M. Gorospe, N.J. Holbrook, Gadd45 is not required for activation of c-Jun N-terminal kinase or p38 during acute stress, J. Biol. Chem. 274 (1999) 29599–29602.
[25] C.Y. Kuan, D.D. Yang, D.R. Samanta Roy, R.J. Davis, P. Rakic, R.A. Flavell, The Jnk1 and Jnk2 protein kinases are required for regional specific apoptosis during early brain development, Neuron 22 (1999) 667–676.
[26] K. Sabapathy, W. Jochum, K. Hochedlinger, L. Chang, M. Karin, E.F. Wagner, Defective neural tube morphogenesis and altered apoptosis in the absence of both JNK1 and JNK2, Mech. Dev. 89 (1999) 115–124.
[27] H. Chi, M.R. Sarkisian, P. Rakic, R.A. Flavell, Loss of mitogen-activated protein kinase kinase kinase 4 (MEKK4) results in enhanced apoptosis and defective neural tube development, Proc. Natl. Acad. Sci. U. S. A. 102 (2005) 3846–3851.
[28] A.N. Abell, J.A. Rivera-Perez, B.D. Cuevas, M.T. Uhlik, S. Sather, N.L. Johnson, S.K. Minton, J.M. Lauder, A.M. Winter-Vann, K. Nakamura, T. Magnuson, R.R. Vaillancourt, L.E. Heasley, G.L. Johnson, Ablation of MEKK4 kinase activity causes neurulation and skeletal patterning defects in the mouse embryo, Mol. Cell. Biol. 25 (2005) 8948–8959.
[29] I. Ivankovic-Dikic, E. Gronroos, A. Blaukat, B.U. Barth, I. Dikic, Pyk2 and FAK regulate neurite outgrowth induced by growth factors and integrins, Nat. Cell Biol. 2 (2000) 574–581.
[30] D.J. Webb, M.J. Schroeder, C.J. Brame, L. Whitmore, J. Shabanowitz, D.F. Hunt, A.R. Horwitz, Paxillin phosphorylation sites mapped by mass spectrometry, J. Cell Sci. 118 (Part 21) (2005) 4925–4929.
[31] C. Huang, C.H. Borchers, M.D. Schaller, K. Jacobson, Phosphorylation of paxillin by p38MAPK is involved in the neurite extension of PC-12 cells, J. Cell Biol. 164 (2004) 593–602.
[32] X. Cai, M. Li, J. Vrana, M.D. Schaller, Glycogen synthase kinase 3- and extracellular signal-regulated kinase-dependent phosphorylation of paxillin regulates cytoskeletal rearrangement, Mol. Cell. Biol. 26 (2006) 2857–2868.

Available online at www.sciencedirect.com
ScienceDirect
Biochemical and Biophysical Research Communications 356 (2007) 739–744
BBRC
www.elsevier.com/locate/ybbrc

Estimation of the embryotoxic effect of CBZ using an ES cell differentiation system

Mayu Murabe, Junji Yamauchi, Yoko Fujiwara, Yuki Miyamoto, Masami Hiroyama, Atsushi Sanbe, Akito Tanoue *

Department of Pharmacology, National Research Institute for Child Health and Development, 2-10-1 Oukura, Setagaya, Tokyo 157-8535, Japan

Received 5 March 2007
Available online 19 March 2007

Abstract

Carbamazepine (CBZ) is one of the most commonly prescribed antiepileptic drugs (AEDs). However, a higher rate of congenital anomalies has been found in infants of mothers treated with CBZ during early pregnancy. Here, we characterize the effects of CBZ using a mouse ES cell differentiation system. The analysis of tissue-specific gene markers showed that CBZ induced early endodermal and mesodermal differentiation but inhibited differentiation of later stages. CBZ also induced ectodermal development, and there was evidence of neural differentiation as ES cells with an immature neuronal phenotype were observed. In contrast, valproic acid (VPA), another anticonvulsant drug, was previously shown to be able to induce ES cells to differentiate into neurons with a mature appearance. CBZ was less cytotoxic to ES cells than VPA. The *in vitro* ES cell assay system has the potential to provide a rapid and accurate approach for estimating the *in vivo* embryotoxicity of therapeutic drugs.

Keywords: Embryotoxicity; Antiepileptic drugs (AEDs); Carbamazepine (CBZ); Valproic acid (VPA)

Epilepsy is one of the most common neurological disorders. It is estimated that about 50 million people worldwide have this disorder [1]. With appropriate antiepileptic drug (AED) therapy, various types of epilepsy-associated seizure can be almost completely controlled in about 75% of patients [2]. Carbamazepine (CBZ) is one of the most widely used AEDs, and is also used in the treatment of neuropathic pains and psychiatric disorders [3,4]. Although treatment with CBZ is usually effective and safe, 30–40% of epileptic patients do not respond satisfactorily [5]. In some cases, CBZ may cause adverse effects. Acute toxicity of CBZ at therapeutic doses mainly involves the central nervous system (CNS) and the gastrointestinal system. In addition, long-term treatment with CBZ may modify plasma lipids, reduce the number of white blood cells, and induce several allergic reactions [4].

CBZ is also known to be a teratogen [6,7]. Therapy of pregnant women with CBZ increases the rate of congenital anomalies in the fetus, in particular neural tube defects (NTDs), cardiovascular and urinary tract anomalies, and cleft palate. CBZ also induces a pattern of minor congenital anomalies and developmental retardation [6,8]. CBZ is structurally similar to tricyclic antidepressants, but shares remarkably similar clinical features to the structurally unrelated AED, valproic acid (VPA), which has a short-chained fatty acid structure [9,10]. VPA is considered to have the highest teratogenic potential of all AEDs, causing a rate of NTDs of about 2% and an increase of 4–8% in major congenital anomalies [11–13].

CBZ is embryotoxic but is less teratogenic than VPA. It causes about 0.5–1% spina bifida (NTD) and 1.5–2.0% cardiovascular anomalies [13]. In our previous study, we characterized the tissue-specific embryotoxicity of VPA using an assay system involving differentiation of mouse embryonic stem (ES) cells [14]. ES cells are undifferentiated pluripotent cells capable of developing into differentiated cell

* Corresponding author. Fax: +81 3 5494 7057.
E-mail address: atanoue@nch.go.jp (A. Tanoue).

0006-291X/$ - see front matter © 2007 Elsevier Inc. All rights reserved.
doi:10.1016/j.bbrc.2007.03.063

types of endodermal, mesodermal, and ectodermal lineages. Our *in vitro* ES cell differentiation assay system is a simple procedure that can be performed rapidly (within 10 days). Through analysis of tissue-specific markers and observation of cell morphologies, we showed that VPA was a potent inhibitor of mesodermal and endodermal development but promoted neuronal differentiation in a lineage-specific manner [14]. Here, we sought to use this system to characterize the tissue-specific, embryotoxic effects of CBZ on developmental processes. Analysis of the expression levels of marker genes showed that although there was dose-dependent expression of early stage differentiation markers, those of later stages were inhibited in a higher concentration over the therapeutic range.

CBZ also induced differentiation of neural cells, an ectodermal cell lineage. When the expression profiles of neural cell gene markers after CBZ treatment were compared with those after VPA, we found that the expression level of an early differentiation marker induced by CBZ was higher than after VPA. In contrast, expression of later stage differentiation markers was lower after CBZ treatment than VPA. Most of the neuronal cells induced by CBZ were neurons with an immature shape that either lacked nerve processes or had small processes. In contrast, VPA induced neuronal cells with a mature shape and long nerve processes. Finally, in light of the differences of *in vivo* embryotoxic effects between CBZ and VPA, our results with the *in vitro* mouse ES cell assay system have confirmed the sensitivity of the system and show that it will be of value for distinguishing fine differences in *in vivo* embryotoxicity of therapeutic drugs.

Methods

ES cell culture and differentiation. Mouse ES cells (R1) were maintained and used for induction of differentiation as previously described [14,15]. ES cells were grown on gelatin-coated tissue culture dishes in a standard ES cell culture medium (D-MEM supplemented with 10% FCS, 2 mM glutamine, 0.1 mM non-essential amino acids, 0.1 mM β-mercaptoethanol, 1000 U/ml LIF (Chemicon, Temecula, CA), 50 U/ml penicillin G, and 50 μg/ml streptomycin). R1 ES cell differentiation was carried out as described previously [14,16]. In brief, ES cells were suspended in an ES-differentiation medium (D-MEM supplemented with 20% FCS, 2 mM glutamine, 0.1 mM non-essential amino acids, 0.1 mM β-mercaptoethanol, 50 U/ml penicillin G, and 50 μg/ml streptomycin) and cultured in hanging drops ($n = 500$) as aggregates (called embryoid bodies, EBs) for 3 days. The EBs were transferred into a suspension medium and cultured for 2 days. They were then plated onto a 24-well tissue culture plate and incubated for 5 additional days. To estimate efficiency of differentiation of ES cells into cardiomyocytes, cultures were analyzed under an inverted phase-contrast microscope (Nikon, Tokyo, Japan) for the distinctive beating movements of differentiated cardiomyocytes.

RNA isolation, cDNA synthesis, RT-PCR, and quantitative RT-PCR. RNA isolation, cDNA synthesis, RT-PCR, and quantitative RT-PCR were performed as described previously [14]. Total RNA was extracted from samples on days 5 and 7 of the differentiation assay. cDNA was synthesized using 3 μg of RNA. To analyze the relative expression of different mRNAs, the amount of cDNA was normalized against ubiquitously expressed GAPDH mRNA. PCR was carried out using an Ex-Taq kit (Takara Bio, Shiga, Japan) according to the manufacturer's standard protocol. For quantitative RT-PCR, gene expression was assessed by real-time PCR with the use of a 7900HT Fast Real-Time PCR System (Applied Biosystems, Foster City, CA). The reaction mixtures contained 1 μl of template cDNA. Duplicate assays were carried out for each sample. The relative expression of each tissue-specific gene marker was calculated after normalization with the housekeeping gene GAPDH. The primer sequences are given in Table 1; the primers for GAPDH were purchased from Applied Biosystems (Foster City, CA).

Immunocytochemistry. On day 3 of the differentiation assay, several EBs were cultured on gelatin-coated glass-based 60 mm dishes. The culture medium was changed on day 5, and the cells were fixed in 4% paraformaldehyde on day 10. The fixed EBs were rinsed with PBS, and blocked in PBS containing 1% BSA, 0.1% gelatin, and 0.1% Tween 20 for 1 h at room temperature. The cells were incubated at 4 °C overnight with the anti-βIII-tubulin antibody (Sigma–Aldrich (St. Louis, MO), mouse IgG, 1:500). After washing with PBS, the cells were incubated for 1 h at room temperature with a secondary antibody conjugated with Alexa 488 (Invitrogen, Carlsbad, CA). The cells were washed with PBS, mounted on glass microscope dishes in Vectashield mounting medium with DAPI (Vector Laboratories, Burlingame, CA), and examined with an FV500 confocal laser-scanning microscope (Olympus, Tokyo, Japan).

Cytotoxicity assay. The cytotoxicity assay was performed as described in our previous report [14]. In brief, ES cells and NIH-3T3 fibroblasts

Table 1
PCR primers used in this study for the detection of tissue-specific marker gene expression

Gene	Sequences (5′–3′)		Product length (bp)
	Forward	Reverse	
Oct4	GGTGGAGGAAGCCGACAAC	TTCGGGCACTTCAGAAACATG	141
Sox2	AGATGCACAACTCGGAGATCAG	CCGCGGCCGGTATTTATAAT	146
BMP4	CTGCCGTCGCCATTCACTAT	TGGCATGGTTGGTTGAGTTG	146
Nkx2.5	CCAAGTGCTCTCCTGCTTTCC	CCATCCGTCTCGGCTTTGT	148
ANF	CGGTGTCCAACACAGATCTG	TCTCTCAGAGGTGGGTTGAC	187
GATA6	CGGTCATTACCTGTGCAATG	GCATTTCTACGCCATAAGGTA	159
TTR	GTCCTCTGATGGTCAAAGTC	TCCAGTTCTACTCTGTACAC	193
HNF1	AGCCGCAGAACCTTATCATG	GGTTGGTGTCTGTGATCAAC	390
ALB	GGAACTTGCCAAGTACATGTGTGA	CAGCAATGGCAGGCAGATC	146
Nestin	TGCATTTCCTTGGGATACCAG	CTTCAGAAAGGCTGTCACAGGAG	122
Synaptophysin	GTGGAGTGTGCCAACAAGAC	ATTCAGCCGAGGAGGAGTAG	158
NFH	AGGACCGTCATCAGGCAGACATTGC	GACCAAAGCCAATCCGACACTCTTC	201
GFAP	TGCCACGCTTCTCCTTGTCT	GCTAGCAAAGCGGTCATTGAG	146
Olig2	TGCGCCTGAAGATCAACAG	CATCTCCTCCAGCGAGTTG	182
DM20	TGAAGCTCTTCACTGGTACAG	GTCTTGTAGTCGCCAAAGAT	207

(1×10^4 cells/ml) were seeded in a volume of 50 μl in a well of a 96-well flat-bottomed tissue culture microtiter plate and incubated for 2 h. After incubation, 150 μl of culture medium containing the appropriate dilution of the test chemical was added. On days 3 and 5 of culture, the medium was changed. On day 10, the methylthiazolyldiphenyl-tetrazolium bromide (MTT) cytotoxicity assay [17] was carried out [14,16]. Representative results from three separate experiments are shown in Fig. 3B. For morphological observations, samples on day 5 were examined using a Hoffman differential interference contrast microscope.

Results and discussions

Effects of CBZ on ES cell differentiation

First, the tissue-specific effects of CBZ in the ES cell differentiation system were characterized at the molecular level. We used real-time RT-PCR on samples from day 5 of culture to determine the expression levels of tissue-specific genes in undifferentiated cells, and in cells differentiating into endodermal and mesodermal lineages (Fig. 1). The expression levels of Sox2 and Oct4 (undifferentiated markers) increased at high CBZ concentrations (Fig. 1A). In the differentiating endodermal lineage, only the expression level of the primitive marker, GATA6, increased (Fig. 1B); the expression levels of the markers of late differentiation stages, TTR and HNF1, decreased in a concentration-dependent manner. Albumin (ALB), a definitive endodermal hepatic marker, was not detected, suggesting that CBZ promoted initial endodermal differentiation but inhibited differentiation into mature endodermal lineages. In the mesodermal lineage, the expression level of the primitive marker, BMP4, increased in a dose-dependent manner (Fig. 1C-1). The expression level of an early cardiac marker, Nkx2.5, showed a slight increase. However, expression of the later stage cardiac marker, ANF, was reduced in a concentration-dependent manner. Under the same culture conditions but omitting CBZ, cardiomyocytes normally differentiate from EBs. We screened for cardiomyocyte differentiation at different concentrations of CBZ. We found that CBZ decreased the rate of undifferentiated ES cells differentiating to cardiomyocytes in a dose-dependent manner (Fig. 1C-2). Thus, based on the gene expression data and rates of cardiomyocyte differentiation, CBZ promoted the initial differentiation into mesodermal lineages, including primitive cardiomyocytes, but inhibited later differentiation into the mature mesodermal lineages. Recently, we reported on the embryotoxicity of VPA using the same ES cell differentiation system [14]. Similar to the observations described here for CBZ, the expression levels of Sox2 and Oct4 (undifferentiated markers) were elevated at high VPA concentrations. In contrast, in cells differentiating into endodermal and mesodermal lineages, CBZ and VPA showed different effects. VPA inhibited the expression levels of almost all markers in all stages of endodermal and mesodermal differentiation, whereas CBZ inhibited expression only at later stages and induced expression in early stages of endodermal and mesodermal differentiation.

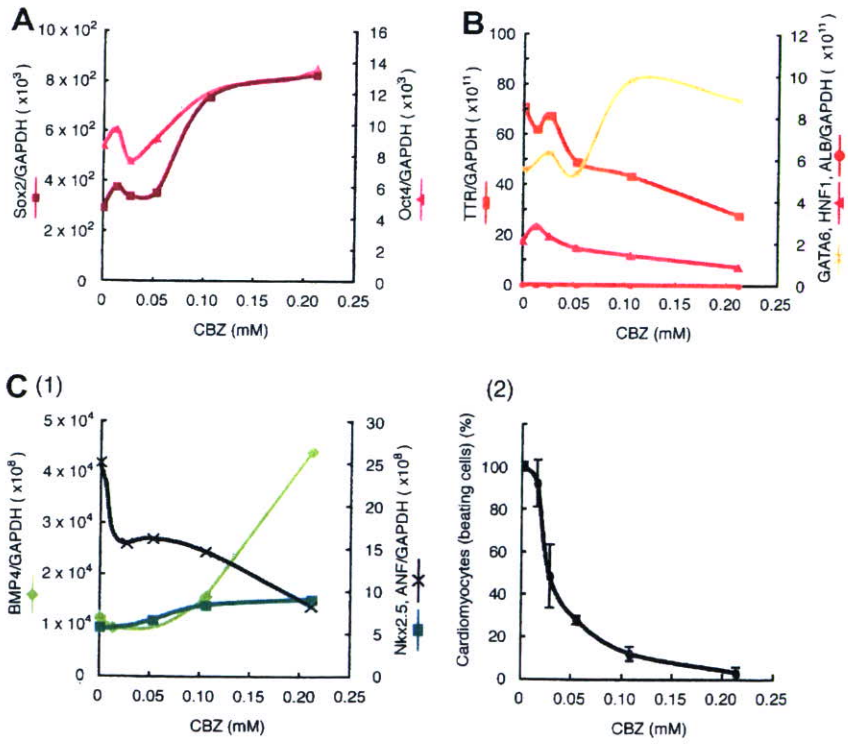

Fig. 1. CBZ embryotoxicity: gene expression profiles in the undifferentiated state and in the differentiating mesodermal and endodermal lineages. The expression levels of the markers of the undifferentiated state, Sox2 and Oct4 (A), endodermal markers, GATA6, TTR, HNF1, and ALB (B), and mesodermal markers, BMP4, Nkx2.5, and ANF (C-1), were quantified at each concentration of CBZ with real-time RT-PCR. The frequencies of cardiomyocytes, identified by their distinctive beating movement, derived from ES cells were quantified at each concentration of CBZ (C-2).